European Journal of Medicinal Chemistry 92 (2015) 784–798

Contents lists available at ScienceDirect

European Journal of Medicinal Chemistry

journal homepage: http://www.elsevier.com/locate/ejmech

Original article

A facile and novel synthesis of N^2-, C^6-substituted pyrazolo[3,4-*d*] pyrimidine-4 carboxylate derivatives as adenosine receptor antagonists

G. Venkatesan [a], P. Paira [b], S.L. Cheong [a], S. Federico [c, *], K.N. Klotz [d], G. Spalluto [c, *], G. Pastorin [a, *]

[a] Department of Pharmacy, National University of Singapore, 3 Science Drive 2, Singapore 117543, Singapore
[b] Pharmaceutical Chemistry Division, School of Advance Science, Vellore Institute of Technology University, Vellore 632014, Tamilnadu, India
[c] Dipartimento di Scienze Chimiche e Farmaceutiche, Università degli Studi di Trieste, Piazzale Europa 1, Trieste 34128, Italy
[d] Institut für Pharmakologie und Toxikologie, Universität Würzburg, Versbacher Strasse 9, Würzburg 97078, Germany

ARTICLE INFO

Article history:
Received 7 November 2014
Received in revised form
21 January 2015
Accepted 22 January 2015
Available online 22 January 2015

Keywords:
Pyrazolo[3,4-*d*]pyrimidine
Carboxylate derivatives
Adenosine receptor antagonists
Homology modeling
Molecular docking
Structure-affinity relationship

ABSTRACT

An efficient synthetic procedure was adopted to synthesize a series of new molecules containing the pyrazolo[3,4-*d*]pyrimidine (PP) scaffold, which have been evaluated as promising human adenosine receptor (AR) antagonists. The effect of substitutions at the N^2, C^4 and C^6 positions of PPs on the affinity and selectivity towards the adenosine receptors were explored. Most of the pyrazolo[3,4-*d*]pyrimidine-4-carboxylates displayed from moderate to good affinity at the human A_3AR (hA_3AR), as indicated by the low micromolar range of K_i values (K_i hA_3AR = 0.7–34 μM). In particular, compounds **60** and **62** displayed good affinity at the hA_3AR (**60**, K_i hA_3AR = 2.2 μM and **62**, K_i hA_3AR = 2.9 μM) and selectivity towards the other AR subtypes (**60**, >46-fold selective and **62**, >34-fold selective, respectively). In view of these results, these novel PP analogues were docked both in the crystallographic structure of the hA_{2A}AR and in a homology model of the hA_3AR in order to support the structure activity relationship (SAR) analysis. These preliminary results demonstrated that pyrazolo[3,4-*d*]pyrimidine can be considered a promising scaffold to obtain new molecules with potent hA_3AR antagonist activity.

1. Introduction

Adenosine is a nucleoside made up of adenine attached to a ribose moiety through a β-N^9-glycosidic linkage. In our body, adenosine acts as an endogenous modulator that regulates many physiological processes through activation of specific human adenosine receptors (hARs) [1–3]. The ARs are generally categorized into four subtypes, namely A_1, A_{2A}, A_{2B} and A_3 ARs [4,5]. All of these ARs possess their own distinct tissue localization, biochemistry and pharmacological function. The diverse physiological functions regulated by the ARs highlight the significant benefits of developing new therapeutics to modulate these receptors. Nevertheless, the ubiquitous distribution of ARs in mammalian cell types, the existence of four distinct subtypes together with the variability of physiological responses indicate the importance of obtaining potential ligands that are highly selective in their action [6,7].

Among the four AR subtypes, the A_3 receptor has been shown to be involved in several patho-physiological conditions that occur in the central nervous and cardiovascular systems, as well as in inflammatory disorders and cancer [8]. Several research groups have made intense efforts in exploring potent and selective ligands for the A_3AR subtype over the past two decades. To date, different classes of compounds with various chemical scaffolds have been successfully synthesized and tested as A_3AR antagonists [8,9]. In particular, our group has focused on the design and synthesis of derivatives bearing the tricyclic pyrazolo[4,3-*e*]1,2,4-triazolo[1,5-*c*] pyrimidine (PTP) scaffold (Compound **1**, Fig. 1), which has resulted in series of compounds with very good binding affinity at the hA_3AR and high selectivity against the other AR subtypes [10–17]. However, in the case of the PTP scaffold and also in most of the

Abbreviations: hA_3AR, human A_3 adenosine receptor; SAR, structure-activity relationship; PTP, pyrazolo[4,3-*e*]1,2,4-triazolo[1,5-*c*]pyrimidine; PP, pyrazolo[3,4-*d*]pyrimidine.

* Corresponding authors.
E-mail address: phapg@nus.edu.sg (G. Pastorin).

http://dx.doi.org/10.1016/j.ejmech.2015.01.046
0223-5234/

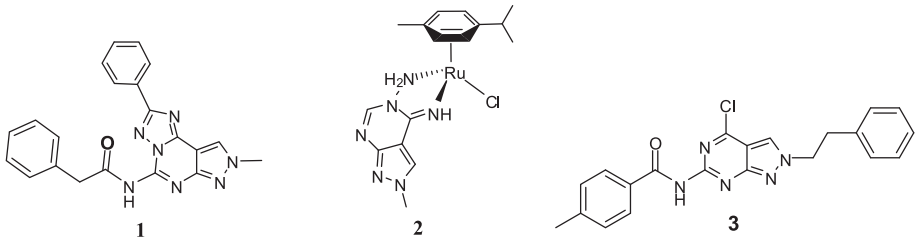

Fig. 1. Examples of hA$_3$AR antagonists.

tricyclic heterocyclic derivatives described in the literature, they are associated with a number of limitations such as complex synthetic schemes, time-consuming reactions, low yields, as well as high molecular weight and lipophilicity which affect the ADME properties [10–13,18]. As such, these observations suggest the need to extend further investigations on different heterocyclic structures in order to overcome these limitations while maintaining or improving the affinity and selectivity towards the hA$_3$AR.

In our initial attempt to introduce some structural diversity in the main PTP scaffold without loosing affinity at the hA$_3$AR, we investigated a series of Ru^{II}-arene complexes containing the (PP) scaffold (Compound **2**, Fig. 1) as chelating ligand, with the aim to explore the effect of altering bulky groups at the 2-aryltriazole position of the PTP scaffold towards binding affinity at the hA$_3$AR, and to overcome the solubility limitations of the PTP analogues [19]. From the study, it was noticed that the newly synthesized PP-Ru^{II}-arene complexes displayed good aqueous solubility and stability. However, the sterically hindered Ru^{II}-arene complexes exhibited affinity in the high micromolar range at the hA$_3$AR and poor selectivity towards the other AR subtypes. In a more recent study we have applied a different molecular simplification strategy [20]. The pyrazolo[3,4-*d*]pyrimidine scaffold was maintained because it represents the core domain of PTP, which interacts with the AR binding pocket. Furthermore, we have introduced various substituents with different lipophilicity and steric hindrance at the N^2 position, which corresponds to the N^8 position of the PTP nucleus and where small alkyl groups gave good affinity at the hA$_3$AR [21]. Benzamido or phenylacetamido moieties were inserted at the C^6 position, such as at the C^5 position of the PTP scaffold [22] in order to confer potency and selectivity at the hA$_3$AR. Finally, at the C^4 position, a chlorine atom was chosen for its restricted rotation, with the aim to enable the pyrazolo[3,4-*d*]pyrimidine to attain the same binding pose of PTP (Compound **3**, Fig. 1) [20]. However, also in this case we obtained derivatives with affinity in the high micromolar range and displaying a poor selectivity profile. Surprisingly, a structural modification on the 4-chloro group through substitution with the rotatable ethyl ester substituent successfully improved the binding affinity and selectivity profiles at the hA$_3$AR of the new derivatives [20]. In fact, compounds **4** and **5** displayed affinities at the hA$_3$AR in the low or even submicromolar range (**4**, K_i hA$_3$AR = 1.3 μM and **5**, K_i hA$_3$AR = 0.9 μM) (Fig. 2).

In view of the good results obtained in terms of affinity and selectivity at the hA$_3$AR, in the present study we decided to expand the ethyl 4-carboxylate-PP series (**46**–**69**). We have synthesised new PP analogues, where the ethyl ester moiety was maintained at the C^4 position, while N^2 alkyl and C^6 amido substituents (that were present at the equivalent N^8 and N^5 position of PTP derivatives [21,22] were introduced in order to explore their effect in terms of affinity and selectivity at the hA$_3$AR. Overall, the main aim of the project was to synthesize PP derivatives with good affinity and selectivity at the hA$_3$ subtype in order to obtain hA$_3$AR antagonists

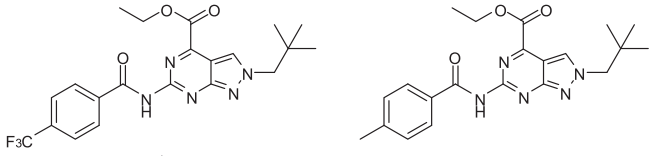

Fig. 2. Pyrazolo[3,4-*d*]pyrimidines (PP) as hA$_3$AR antagonists.

with easier synthetic procedures and better ADME properties than the potent tricyclic hA$_3$AR antagonists reported in the literature [18].

2. Results and discussion

2.1. Chemistry

In this new series of pyrazolo[3,4-*d*]pyrimidine (PP) derivatives, we have rationally designed and incorporated various substituents at the N^2 (lipophilic alkyl and aralkyl chains), C^6 (amino, substituted benzamido and phenylacetamido groups) and C^4 (ester substituents) positions of the bicyclic scaffold in order to examine their effects on the binding affinity and selectivity profiles. Based on the synthetic steps illustrated in Schemes 1 and 2, the new series of 6-substituted ethyl 2-(ar)alkyl-2*H*-pyrazolo[3,4-*d*]pyrimidine-4-carboxylate derivatives (**42**–**69**) have been successfully synthesized and characterized.

As reported in literature, the alkylation of 3-amino-4-pyrazole carbonitrile was carried out with alkyl or aralkyl iodide or bromide in dry DMF using dry potassium carbonate as a weak base, which led to N^1 substituted regioisomer (**6**–**9**) as a major product [10,19,20].

The 3-amino-N^1-substituted-4-pyrazolo carbonitriles (**6**–**9**) were then hydrolysed to corresponding carboxamides (**10**–**13**) under acidic conditions at low temperature for 30 min, followed by stirring at ambient conditions for 5 h (Scheme 1). The conversion of nitrile to amide was confirmed by ^{1}H NMR analysis and two broad singlets were observed for CONH$_2$ proton as specified in the literature [23–26]. Among the carboxamide derivatives (**10**–**13**), compound **10** has been reported in the literature [27] and compound **11** is commercially available.

Yamazaki and collaborators have described the synthesis of guanosine derivatives by condensation of 4-cyanamido-1*H*-imidazole-5-carboxamide with benzoyl isothiocyanate, followed by methylation and ring closure [28]. Similar synthetic steps were adopted in our scheme for the synthesis of benzoylthiouriedo

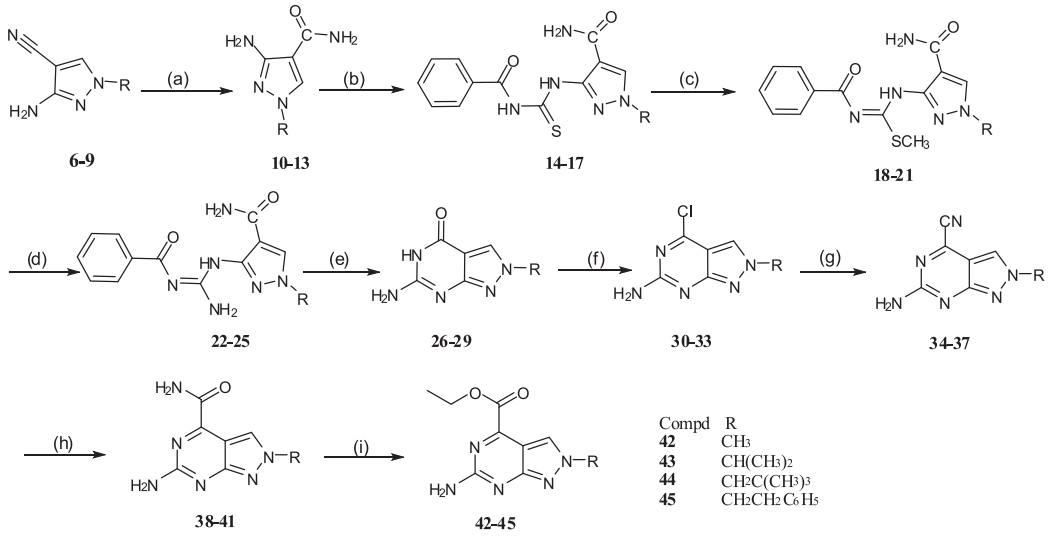

Scheme 1. General procedure for the synthesis of the 6-substituted ethyl 2-(ar)alkyl-2*H*-pyrazolo[3,4-*d*]pyrimidine-4-carboxylate derivatives. Reagents: (a) conc. H_2SO_4, 0 °C to rt, 5 h; (b) C6H5CONCS, acetone, reflux, 12 h; (c) CH_3I, 0.1 N NaOH, rt, 3 h; (d) 2% aq. NH_3, DMF, 120 °C sealed tube, 3 h; (e) 1 N NaOH, reflux, 12 h; (f) $POCl_3$, dimethylaniline, reflux, 24 h; (g) NaCN, p-toluene sulfinate sodium, DMF, 80 °C, 2 h; (h) K_2CO_3, 30% H_2O_2, rt, 1 h; (i) EtOH, conc. H_2SO_4, reflux, 12 h.

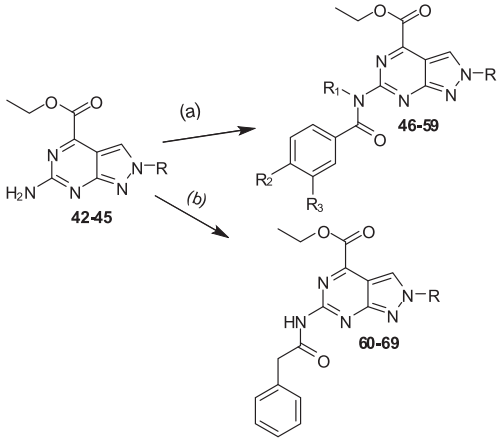

No	R	R_1	R_2	R_3
42	**CH_3**	-	-	-
43	**$CH(CH_3)_2$**	-	-	-
44	**$CH_2C(CH_3)_3$**	-	-	-
45	**$CH_2CH_2C_6H_5$**	-	-	-
46	**CH_3**	H	H	H
47	**CH_3**	H	F	H
48	**CH_3**	H	CF_3	H
49	**CH_3**	H	CH_3	H
50	**$CH(CH_3)_2$**	H	H	H
51	**$CH(CH_3)_2$**	H	F	H
52	**$CH(CH_3)_2$**	H	CF_3	H
53	**$CH(CH_3)_2$**	H	CH_3	H
54	**$CH_2C(CH_3)_3$**	H	F	H
55	**$CH_2CH_2C_6H_5$**	H	H	H

No	R	R_1	R_2	R_3
56	**$CH_2CH_2C_6H_5$**	H	F	H
57	**$CH_2CH_2C_6H_5$**	H	CF_3	H
58	**$CH_2CH_2C_6H_5$**	H	CH_3	H
59	**$CH_2CH_2C_6H_5$**	H	Br	H
60	**$CH_2CH_2C_6H_5$**	H	Cl	Cl
61	**CH_3**	C_6H_5CO	H	H
62	**CH_3**	4-Br-C_6H_5CO	Br	H
63	**CH_3**	3,4-F-C_6H_5CO	F	F
64	**$CH(CH_3)_2$**	C_6H_5CO	H	H
65	**$CH_2CH_2C_6H_5$**	C_6H_5CO	H	H
66	**CH_3**	-	-	-
67	**$CH(CH_3)_2$**	-	-	-
68	**$CH_2C(CH_3)_3$**	-	-	-
69	**$CH_2CH_2C_6H_5$**	-	-	-

Scheme 2. General procedure for the synthesis of the 6-substituted ethyl 2-(ar)alkyl-2*H*-pyrazolo[3,4-*d*]pyrimidine-4-carboxylate derivatives. Reagents : (a) substituted benzoyl chloride, DIPEA, toluene, 120 °C, reflux, 24 h ; (b) phenyacetyl chloride, DIPEA, toluene, 120 °C, reflux, 24 h.

derivatives **14**–**17** with some modifications. As per methods reported in the literature, the carboxamide (**10**–**13**) was initially reacted with benzoyl isothiocyanate in water at room temperature. However, the corresponding benzoylthioureido derivatives were not obtained. Nevertheless, when the reaction was carried out in 50% aqueous acetone at high temperature (80–100 °C), thioureido derivatives were obtained with low yield, probably due to partial decomposition of benzoyl isothiocyanate in aqueous conditions. As such, the reaction was performed in dry acetone, followed by condensation with benzoyl isothiocyanate under reflux conditions for 12 h. Upon cooling, the benzoylthioureido derivatives (**14**–**17**) were obtained as yellow solids with good yields.

It is known that the methylmercapto group activated by the electron-withdrawing nature of benzoyl group would be more reactive. Hence, the methylation reaction was performed by treating intermediate compounds **14**–**17** with methyliodide in aqueous sodium hydroxide solution at ambient temperature for 3 h to obtain methylthio derivatives (**18**–**21**). After adjusting the pH to 6, the corresponding carbamidothioates (**18**–**21**) were obtained as white solids.

Subsequently, the nucleophilic substitution of methylmercapto group by NH_2 was carried out in DMF containing 2% ammonia with vigorous heating in a sealed tube. As expected, the electron-poor isothiourea carbon was readily attacked by the nucleophile NH_2 to afford benzoylguanidino derivatives **22**–**25**. The completion of the reaction was confirmed by the odour of methyl mercaptan from the reaction vessel. Unfortunately, the synthesized compounds **22**–**25** were insoluble in any solvent. Hence, they were directly taken to the next reaction. Afterwards, benzoyl guanidines **22**–**25** were easily cyclized to 6-amino-2-substituted-2*H*-pyrazolo[3,4-*d*] pyrimidin-4(5*H*)-one derivatives (**26**–**29**) upon treatment with 1 N sodium hydroxide under reflux conditions. Upon cooling, the pH of the reaction mixture was adjusted to 6 to obtain a precipitate. For this reaction, the nitrogen atom of the carbamoyl group attacked the carbon atom of the methenamine group, followed by elimination of ammonia and benzoic acid. The traces of benzoic acid were easily separated by stirring the product in hot ethanol. Compounds **26**–**29** were obtained in higher yields (ranging from 68 to 81 %) [20].

Chlorination of the 6-amino-2-alkyl-2*H*-pyrazolo[3,4-*d*]pyrimidin-4(5*H*)-ones (**26**–**29**) was carried out with phosphoryl trichloride ($POCl_3$) in the presence of *N*,*N*-dimethyl aniline under reflux condition for 24 h [20]. After completion of the reaction, the excess of $POCl_3$ was carefully removed and the crude product was purified by column chromatography to obtain the corresponding chloro analogues (**30**–**33**) as solids. Compounds **34**–**37** were prepared by treating chloro derivatives **30**–**33** with sodium cyanide in dry DMF in the presence of sodium *p*-toluene sulfinate as catalyst at 80 °C for 2 h. The nitrile groups were detected by the presence of CN peak at 115 ppm in ^{13}C NMR spectra and also confirmed by the presence of CN peak between 2250 and 2260 cm^{-1} in the IR spectra. The following hydrolysis of the nitrile group was carried out based on the literature method called “Radziszewski reaction”, by using aqueous hydrogen peroxide and aqueous potassium carbonate in cold or hot conditions [29]. However, the product was obtained in low yields. Conversely, when the reaction was carried out at room temperature, the resulting carbamides (**38**–**41**) were obtained in good yield. Subsequently, these intermediate compounds (**38**–**41**) were esterified in the presence of conc. H_2SO_4 with absolute ethanol under reflux conditions to afford the corresponding carboxylates **42**–**45** as solids.

Acylation of compounds **42**–**45** was carried out as described in Scheme 2. 3 equivalents of substituted benzoyl chlorides or phenylacetyl chloride and diisopropylethylamine (DIPEA) were used to obtain monoacylated compounds **46**–**60**, and **66**–**69**, respectively.

Instead, disubstituted derivatives (**61**–**65**) were prepared under standard conditions, using 6 equivalents of substituted benzoyl chlorides and DIPEA. Final derivatives were characterized by ^1H NMR, ^{13}C NMR, HMQC NMR and ESI-Mass analysis.

2.2. Structure-affinity relationship study

Pharmacological evaluation was performed for the new series of pyrazolo[3,4-*d*]pyrimidine-4-carboxylate to examine their affinity at all four AR subtypes. The receptor binding affinities of compounds **38**–**69** were determined at the human A_1, A_{2A}, A_3 receptors, while the inhibition of adenylyl cyclase activity was determined for the human A_{2B} receptors (Table 1). Also compounds **4** and **5**, recently reported in our work on the PP series [20] were included in Table 1 as they are structurally related to the new synthesised derivatives of this study and could help to make a more detailed SAR profile of PP derivatives.

Most of the synthesized derivatives showed affinity in the low micromolar range for at least one of the AR subtypes. Their selectivity profile is regulated by substituents present at the N^2, C^4 and C^6 position. Indeed, most of the pyrazolo[3,4-*d*]pyrimidine-4-carboxylates displayed from moderate to good affinity at the hA_3 receptors as indicated by the low micromolar range of K_i values (K_i hA_3AR = 0.7–34 μM) and with some compounds displaying high selectivity (e.g. **60**, hA_1/hA_3 and hA_{2A}/hA_3 >46) towards other AR subtypes. Besides that, all the PP-4-carboxylates were found inactive at the $hA_{2B}AR$. The binding assay results of the analogues bearing various alkyl substitutions (i.e. methyl, isopropyl or neopentyl) or a phenylethyl group at N^2 position were compared to examine the impact of those substitutions on the binding affinity and selectivity profiles at the four AR subtypes (Table 1).

2.2.1. Effect of C^6 free aminosubstitution on binding affinity of PP scaffold

Binding affinity of C^4 amide substituted derivatives (**38**–**41**) bearing a C^6 free amino group were compared to that of the corresponding C^4 ester substituted compounds (**42**–**45**). All of the C^4-amido substituted compounds (**38**–**41**) were shown to exhibit weak affinity towards the hA_3AR (K_i hA_3AR = 16.9–>100 μM) as compared to the C^4-ester compounds (**42**–**45**, K_i hA_3AR = 0.7–30 μM). However, C^4-amido compounds bearing little alkyl moieties at the N^2 position, such as a methyl (**38**) or a propyl (**39**) group, propelled the affinity towards $hA_{2A}AR$ and hA_1AR and displayed up to 11-fold selectivity over the hA_3AR. Conversely, among the C^4-ester derivatives (**42**–**45**), compound **42**, with a methyl group at N^2, displayed the best affinity at the hA_3AR (K_i hA_3AR = 0.7 μM) in the whole series of PP derivatives, together with moderate affinity towards the other receptor subtypes (K_i $hA_{2A}AR$ = 2 μM and K_i hA_1AR = 9.3 μM). On the other hand, compound **43**, with a N^2 isopropyl group, displayed a submicromolar affinity towards the hA_1AR (K_i hA_1AR = 0.9 μM), and 35-fold selectivity over the hA_3AR. So, excepted for the $hA_{2B}AR$, C^4-ester compounds displayed affinity in the micromolar range at all the AR subtypes.

2.2.2. Effect of C^6 acyl substitution on binding affinity of PP scaffold

2.2.2.1. N^2-methyl series. Introduction of a benzoyl or substituted benzoyl group at the C^6 amino moiety of compound **42**, which bears a methyl group at N^2 position, gave rise to compounds with drastically decreased affinity towards the hA_3AR (**46**–**49**, **61** and **63**, with K_i hA_3AR >100 μM). The only exception was observed with compound **62** bearing a 4-bromo-N-(4-bromobenzoyl)-benzamido substitution at C^6 position: this compound, in fact, presented the best combined affinity and selectivity profile among the N^2 small alkyl substituted derivatives (**62**, K_i hA_3AR = 2.9 μM, hA_1/A_3 >34,

Table 1
Binding affinity (K_i) of synthesized compounds at hA_1AR, $hA_{2A}AR$, and hA_3AR; adenylyl cyclase activity at the $hA_{2B}AR$ and selectivity against hA_1AR and $hA_{2A}AR$.

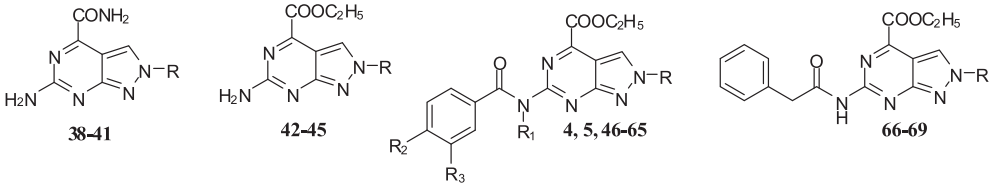

Compd	R	R^1	R^2	R^3	K_i hA_1 (μM)[a]	$K_i hA_{2A}$ (μM)[b]	$K_i hA_{2B}$ (μM)[c]	K_i hA_3 (μM)[d]	Selectivity	
									hA_1/hA_3	hA_{2A}/hA_3
38	CH_3	–	–	–	10.2 (6.2–18.2)	3.0 (1.8–4.9)	>20	>100	>0.10	>0.03
39	$CH(CH_3)_2$	–	–	–	8.2 (5.9–11.3)	9.2 (7.4–11.5)	>20	>100	>0.08	>0.09
40	$CH_2C(CH_3)_3$	–	–	–	>90	>80	>20	19.7 (10.4–37.3)	4.6	4.1
41	$CH_2CH_2C_6H_5$	–	–	–	40.2 (23.6–68.6)	15.7 (9.6–25.8)	>20	32.9 (21.5–50.3)	1.2	0.47
42	CH_3	–	–	–	8.8 (5.4–14.3)	2.0 (1.6–2.4)	>20	0.9 (0.5–1.6)	9.7	2.2
43	$CH(CH_3)_2$	–	–	–	0.9 (0.7–1.1)	2.6 (1.9–3.6)	>10	14.0 (3.2–61.2)	0.06	0.18
44	$CH_2C(CH_3)_3$	–	–	–	4.0 (3.2–5.2)	5.0 (3.0–8.7)	>15	10.4 (5.1–21.0)	0.38	0.48
45	$CH_2CH_2C_6H_5$	–	–	–	3.5 (2.0–5.9)	4.8 (3.4–6.7)	~60	18.1 (10.7–30.5)	0.19	0.26
46	CH_3	H	H	H	14.0 (6.3–31.1)	16.1 (13.8–18.7)	>20	>100	<0.14	<0.16
47	CH_3	H	F	H	>100	11.5 (6.9–19.0)	>20	>100	–	<0.14
48	CH_3	H	CF_3	H	>100	>100	>20	>100	–	–
49	CH_3	H	CH_3	H	>100	11.8 (8.2–16.9)	>20	~100	>1	0.12
50	$CH(CH_3)_2$	H	H	H	4.3 (2.3–8.1)	3.3 (2.9–3.8)	>10	8.6 (3.3–22.3)	0.5	0.4
51	$CH(CH_3)_2$	H	F	H	2.8 (1.8–4.4)	2.8 (1.4–5.5)	>20	5.7 (5.5–5.9)	0.5	0.5
52	$CH(CH_3)_2$	H	CF_3	H	>100	>100	>20	>100	–	–
53	$CH(CH_3)_2$	H	CH_3	H	0.7 (0.5–0.9)	2.3 (1.2–4.3)	>20	28.0 (20.5–38.3)	0.02	0.1
54	$CH_2C(CH_3)_3$	H	F	H	2.7 (1.8–3.9)	5.7 (3.7–8.7)	>20	4.3 (2.9–6.5)	0.62	1.3
4[e]	$CH_2C(CH_3)_3$	H	CF_3	H	>100	>100	>20	1.3 (1.3–1.4)	>77	>77
5[e]	$CH_2C(CH_3)_3$	H	CH_3	H	>100	>90	>20	0.9 (0.7–1.0)	>111	>111
55	$CH_2CH_2C_6H_5$	H	H	H	5.1 (3.8–6.8)	3.7 (3.1–4.4)	>10	12.2 (3.5–42.6)	0.41	0.3
56	$CH_2CH_2C_6H_5$	H	F	H	5.0 (3.5–7.2)	6.1 (4.5–7.0)	>20	6.8 (4.6–10.1)	0.73	0.8
57	$CH_2CH_2C_6H_5$	H	CF_3	H	2.5 (1.4–4.3)	7.5 (5.6–9.7)	>20	5.8 (2.5–13.7)	0.5	1.3
58	$CH_2CH_2C_6H_5$	H	CH_3	H	>100	6.0 (4.4–7.9)	>20	3.0 (2.7–3.4)	>33	2
59	$CH_2CH_2C_6H_5$	H	Br	H	2.6 (2.2–2.9)	4.2 (2.4–7.2)	>20	3.6 (3.5–3.7)	0.72	1.2
60	$CH_2CH_2C_6H_5$	H	Cl	Cl	>100	>100	>20	2.2 (1.4–3.1)	>46	>46
61	CH_3	C_6H_5CO	H	H	>100	>100	>20	>100	–	–
62	CH_3	$(4Br)C_6H_5CO$	Br	H	>100	>100	>20	2.9 (1.9–4.2)	>34	>34
63	CH_3	$(3,4F)C_6H_5CO$	F	F	>100	>100	>20	>100	–	–
64	$CH(CH_3)_2$	C_6H_5CO	H	H	17.7 (11.3–25.7)	>100	>20	5.4 (3.5–7.6)	3.2	>18.5
65	$CH_2CH_2C_6H_5$	C_6H_5CO	H	H	>100	>100	>20	>100	–	–
66	CH_3	–	–	–	5.9 (4.4–7.3)	7.3 (6.2–8.5)	>20	14.6 (9.5–22.3)	0.4	0.5
67	$CH(CH_3)_2$	–	–	–	0.6 (0.3–1.2)	8.8 (7.8–9.9)	>10	13.3 (6.5–27.3)	0.04	0.66
68	$CH_2C(CH_3)_3$	–	–	–	2.7 (1.8–3.9)	5.7 (3.7–8.7)	>20	4.3 (2.9–6.5)	0.62	1.3
69	$CH_2CH_2C_6H_5$	–	–	–	0.6 (0.6–0.7)	2.4 (1.2–4.5)	>10	10.4 (4.3–24.8)	0.05	0.2

[a] Displacement of specific [^{3}H]-2-chloro-6-cyclopentyl adenosine (CCPA) binding at hA_1AR expressed in Chinese Hamster Ovary (CHO) cells (n = 3–6).
[b] Displacement of specific [^{3}H]-5′-*N*-ethylcarboxamido adenosine (NECA) binding at $hA_{2A}AR$ expressed in CHO cells (n = 3–6).
[c] K_i values for inhibition of NECA-stimulated adenylyl cyclase activity in CHO cells (n = 3–6).
[d] Displacement of specific [^{3}H]-2-(1-hexynyl)-N^6-methyl adenosine (HEMADO) binding at hA_3AR expressed in CHO cells (n = 3–6).
[e] [20].

hA_{2A}/hA_3 >34). The reason behind such affinity profile is still unclear, since similar benzoylbenzamido compounds **61** and **62** were shown to be inactive at the hA_3AR (K_i hA_3AR >100 μM). This suggests that a relatively big group at *para* position of dibenzoyl chain, such as a bromo atom, might play an essential role for the improvement of affinity at the hA_3AR.

2.2.2.2. N^2-isopropyl series. On the other hand, benzamido substitution at C^6 position of N^2 isopropyl derivatives (**50**–**53**) showed much improved hA_3 affinity (K_i hA_3AR = 5.3–28.7 μM) as compared to its N^2-methyl counterpart derivatives (**46**–**49**, K_i $hA_3AR \geq 100$ μM), with the exception of compound **52**, which was inactive at all the AR subtypes. Nevertheless, these derivatives (**50**–**53**) showed better affinity at the $hA_{2A}AR$ and hA_1AR, thus resulting in lower selectivity of the compounds. Compound **64**, with a N-benzoylbenzamide at the C^6 position, displayed good hA_3 affinity (K_i hA_3AR = 5.4 μM) and high selectivity (hA_{2A}/hA_3 >19) towards the $hA_{2A}AR$ subtype. In contrast, compound **53**, with *para*-CH_3 benzamido chain at C^6 position, while was almost inactive at the hA_3AR, showed submicromolar affinity towards the hA_1AR (K_i hA_1 = 0.7 μM).

2.2.2.3. N^2-neopentyl series. Notably, N^2 neopentyl analogues with C^6-benzamido substitution displayed the overall best hA_3 affinity (K_i hA_3AR = 0.9–8.1 μM) and selectivity among the other N^2 alkyl and phenylethyl substituted derivatives. The presence of *para*-F group in the benzamido chain led to compound **54**, with hA_3 affinity (K_i hA_3AR = 4.5 μM) comparable to its N^2 isopropyl counterpart (**51**, K_i hA_3AR = 5.7 μM).

When the *para*-F group of benzamide was replaced by a bigger electron withdrawing CF_3 group, the affinity was increased by about 4-fold (**4**, K_i hA_3AR = 1.3 μM) [20] in comparison to compound **54**. In addition, the selectivity towards both $hA_{2A}AR$ and hA_1AR was remarkably improved (**4**, hA_{2A}/hA_3 > 77). Similarly, when *para*-CH_3 group was introduced at the benzamide chain, the hA_3 affinity was further improved (**5**, K_i hA_3AR = 0.9 μM) by 5-fold

in relative to compound **54**. Moreover, compound **5** showed the second best hA_3 affinity and remained the most selective (111-fold against $hA_{2A}AR$ and hA_1AR) in the whole series of PP derivatives [20]. This result suggests that both electron-withdrawing CF_3 and electron-donating CH_3 groups with steric hindrance are essential for the affinity at hA_3AR and selectivity towards the other AR subtypes.

2.2.2.4. N^2 phenylethyl series. Benzamido substitution in the N^2 phenylethyl series (**55**–**60**) improved the hA_3 affinity (K_i hA_3AR = 2.2–9.0 μM) as compared to the free amino counterpart **45** (K_i hA_3AR = 17 μM). On the contrary, dibenzoyl substitution of the amino group at the C^6 position led to compound **65**, which was not active at any of the receptor subtypes. Among these derivatives, unsubstituted benzamide (**55**) showed moderate affinity at the hA_3AR (K_i hA_3AR = 7.4 μM). Surprisingly, electron withdrawing substitution such as F (**56**, K_i hA_3AR = 7.0 μM) and CF_3 (**57**, K_i hA_3AR = 9.0 μM) failed to make any additional impact on the affinity at hA_3AR. Conversely, *para*-CH_3 benzamide (**58**, K_i hA_3AR = 3.0 μM) improved the hA_3AR affinity by around 2.5-fold as compared to the unsubstituted benzamide derivative (**55**) and also strengthened the selectivity against hA_1AR (hA_{2A}/hA_3 > 33). In addition, introduction of a bulky Br group at the *para* position of benzamide (**59**) led to a 2-fold increment in the hA_3AR affinity (K_i hA_3AR = 3.6 μM) in relative to **55**. Similarly, steric dichloro substitution at 3- and 4-position of benzamide (**60**) ameliorated the affinity by >3-fold (K_i hA_3AR = 2.2 μM) as compared to **55**. This compound (**60**) was at least 46 times more selective for hA_3AR against the $hA_{2A}AR$ and hA_1AR.

Throughout the whole N_2 (ar)alkyl series, the presence of lengthy phenylacetamide substitution (**66**–**69**) at the C^6 position did not cause any significant improvement to the affinity (K_i hA_3AR = 7.1–15.2 μM) and selectivity at the hA_3AR. This suggests that phenylacetamido moiety was tolerated in all the AR subtypes in a similar manner. Moreover, compounds **67** (K_i hA_1AR = 0.7 μM) and **69** (K_i hA_1AR = 0.6 μM) showed higher affinity towards the hA_1AR.

As a whole, further ligand modification of the ethyl 4-carboxylate-PP analogues led to the new series of PP derivatives with affinity values towards hA_3AR in the micromolar range. The structure-affinity relationship study showed that substituents at N^2, C^4 and C^6 positions play a key role in modulating the binding affinity at the hA_3AR. In particular, at the N^2 position, neopentyl substitution showed favourable effect on the hA_3AR affinity (**5**, K_i hA_3AR = 0.9 μM). The previously reported compounds **4** and **5** [20] were the best derivatives of the series, showing a good affinity and selectivity towards the hA_3AR. In particular, *para*-CF_3 and *para*-CH_3 groups on the C^6-benzamido moiety seem to be important for the hA_3AR selectivity (**5**; hA_1/hA_3 >111, hA_{2A}/hA_3 >111 and **4**; hA_1/hA_3 >77, hA_{2A}/hA_3 >77). Additionally, C^6-free amino group with N^2 methyl substitution was demonstrated to be vital for the hA_3 affinity (**42**, K_i hA_3AR = 0.7 μM) but not for selectivity, whereas subsequent acylation was detrimental to the affinity of the methyl derivatives (**46**, K_i hA_3AR ≥ 100 μM). In contrast, dibenzamide substituents with steric groups at the *para* position in the N^2 methyl series was essential for hA_3 affinity (**62**, K_i hA_3AR = 2.9 μM) and selectivity (hA_1/hA_3 >34, hA_{2A}/hA_3 >34) against the other AR subtypes. N^2-phenylethyl derivatives (**55**–**60**) displayed good affinity at the hA_3AR, but selectivity was poor, excepted for compound **60**. In fact, the 3,4-dichlorobenzamido substitution led to an enhancement of affinity (**60**, K_i hA_3AR = 2.2 μM) and selectivity (hA_1/hA_3 >46, hA_{2A}/hA_3 >46) towards hA_3AR. Overall, SAR results confirmed the importance of the following substitutions for the hA_3 affinity and selectivity:

i) C^4 ester for conferring affinity;
ii) lipophilic neopentyl group at N^2 position for conferring affinity;
iii) substitution at the aromatic ring of the benzamide at C^6 for conferring selectivity;
iv) N^2 methyl with free amino group or dibenzamide substitution with steric groups (e.g. Br) at C^6 for conferring affinity.

2.3. Molecular docking studies

The molecular docking studies were performed on newly synthesized pyrazolopyrimidine-4-carboxylate derivatives (**38**–**69**) and on the previously reported, structurally related, compounds **4** and **5** [20] to identify hypothetical binding modes and interactions at the hA_3AR, as well as to rationalize the results of the binding data. Docking studies were carried out using molecular operating environment (MOE) programme and all pyrazolo[3,4-*d*]pyrimidine-4-carboxylate derivatives were docked into the orthosteric transmembrane (TM) binding cavities of both hA_3 and hA_{2A} ARs.

Docking simulation at the hA_3AR demonstrated that the binding pattern of the new derivatives varied depending on the substituents at the N^2 and C^6 position of the PP scaffold. Ligand-recognition occurred in the upper region of the TM bundle, and the pyrazolo[3,4-*d*]pyrimidine scaffold was surrounded by TMs 3, 5, 6 and 7. Four different types of interactions were observed and among them hydrophobic interactions and hydrogen bonding interaction seemed to play an essential role for the binding affinity of ligands.

Among the C^6 free amino derivatives, compound **42** was positioned at the centre of the binding pocket on the top of the TM helix (Fig. 3-A). This could be due to the unrotatable nature of the N^2-methyl group, which assisted the ligand to obtain a stable conformation at the centre of the binding pocket.

Moreover, compound **42** also made a stabilizing hydrogen bonding interaction with Asn250, whereas pyrimidine ring of the PP scaffold made π–π stacking interaction with Phe168. On the other hand, other compounds (**43**–**45**) with bulky chains at N^2 position, due to steric hindrance, orientated in a different fashion, which shifted away from the centre and moved towards the TM4. The binding mode of compound **42** inside the $hA_{2A}AR$ was also analysed. Interestingly, the compound occupied the same position as hA_3AR and it retained the vital hydrogen bonding interaction with Asn253 and other hydrophobic interactions with $hA_{2A}AR$. This has led to the poor selectivity of compound **42** over the $hA_{2A}AR$ (K_i hA_3AR = 0.7 μM, K_i $hA_{2A}AR$ = 2.0 μM).

In contrast, acylated compounds of N^2 methyl derivatives (**46**–**49**, **61**) displayed different binding pose at the hA_3AR as compared to compound **42**. The presence of a benzoyl group on the amino group at the C^6 position of the analogues caused the ligands to move away from the centre of the hA_3AR binding pocket, and to orient slightly to the interior towards TM4. This caused the ligands to lose an essential hydrogen bonding interaction with Asn250 and also a π–π stacking interaction with Phe168, which could easily explain the inactivity of these compounds at the hA_3AR subtype. Whereas compound **68**, with lengthy phenylacetamide chain at C^6 position, was able to interact with some of the hydrophobic residues because of the rotatable methylene group, which assisted the ligand to attain a slightly different binding pattern. In fact, compound **68** showed some affinity at the hA_3AR (K_i hA_3AR = 15.2 μM).

In addition, compound **62**, with 4-bromo-N-(4-bromobenzoyl)-benzamido substituent at C^6 position, was positioned at the centre, due to broaden and rotatable nature of the dibenzamide chain (Fig. 3-B). Moreover, this substituted N-benzoylbenzamido chain interacted with hydrophobic residues such as Val72, Ser73, Leu68 and Tyr265. Interestingly, these interactions were not seen with the

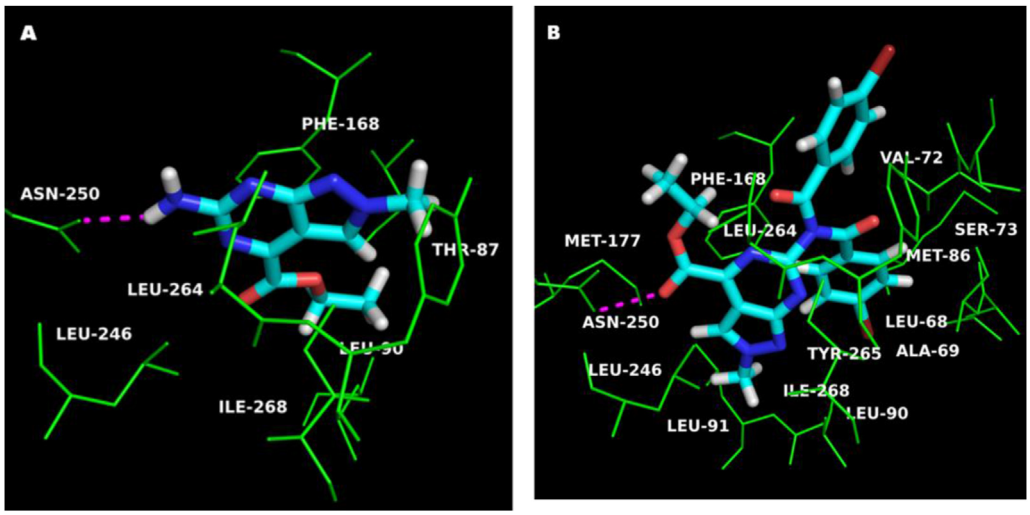

Fig. 3. Hypothetical binding mode of compound **42** (**A**) and compound **62** (**B**) obtained after docking simulations inside the hA_3AR binding site. Poses are viewed from the membrane side facing TM6, TM7, and TM1.

para unsubstituted N-benzoylbenzamido derivatives (compound **61**). Similarly, the ethyl group of the C^4-ester chain of compound **62** interacted with Met177, Leu246, and Leu264, while the basic nucleus of PP made π-π stacking interactions with Phe168. Most importantly, the carbonyl group of the ester substituent made hydrogen bonding interactions with Asn250. This proves the speculation that hA_3AR binding site possesses the maximum spatial tolerability, which can accommodate the broaden diacyl chain with even bulky steric groups (e.g. Br).

Generally, acylated N^2 isopropyl ligands (**50**–**53**, **64**, **67**) moved towards the centre of the binding pocket due to the steric hindrance produced by the isopropyl group, which extended towards the TM4. Ligands were bound in a vertical direction at the centre of the binding pocket and these binding poses are quite different from the one observed for the benzamide derivatives (**46**–**49**) of N^2 methyl group series. The basic scaffold was situated at the centre of the binding pocket and the benzamide chains are extended towards the TM6 and TM7. Due to this close contact with TM helix, the carbonyl group of the ester chains was able to make a hydrogen bonding interaction with Asn250, with exception of compound **52** with steric CF_3 group that created a steric hindrance and made the chain unavailable for the interaction with Asn250 residue.

Interestingly, N^2 neopentyl substituted benzamide compounds (**4**, **5**, **54**) displayed a slightly different binding pose in comparison to compound **42**. Docking analysis of compound **4** and **5** was also reported in our previous work on PP derivatives [20] and, regarding compound **5**, (Fig. 4-A), which was the most potent analogue of the C^4-ester series, it was observed that this compound was placed slightly away from the centre of the binding pocket towards the TM5. In addition, the ester group was oriented towards the TM2 and the phenyl ring of the benzamide pointed towards the ECL2. Due to this reason, compound **5** was able to make three stabilizing hydrogen bonding interactions with Asn250. Similarly, compound **4** shared a close resemblance of the binding pose and was also involved in similar binding interactions. Besides the hydrogen bonding with Asn250, we could observe hydrophobic interactions with residues such as Val169, Ile253, Val259 and Leu264. In particular, Val169, which was not conserved among the AR subtypes, was deemed to influence not only the affinity of a ligand but also its selectivity towards the other AR subtypes [30]. In addition, the neopentyl chain enabled the hydrophobic interaction with Trp243, Leu91, Ser181 and Ser247. The central PP scaffold was involved in a π-π stacking interaction with Phe168, which is considered to be crucial for the hA_3AR but also for the $hA_{2A}AR$ antagonist activity [31,32].

In addition, N^2 phenylethyl benzamide substituted derivatives

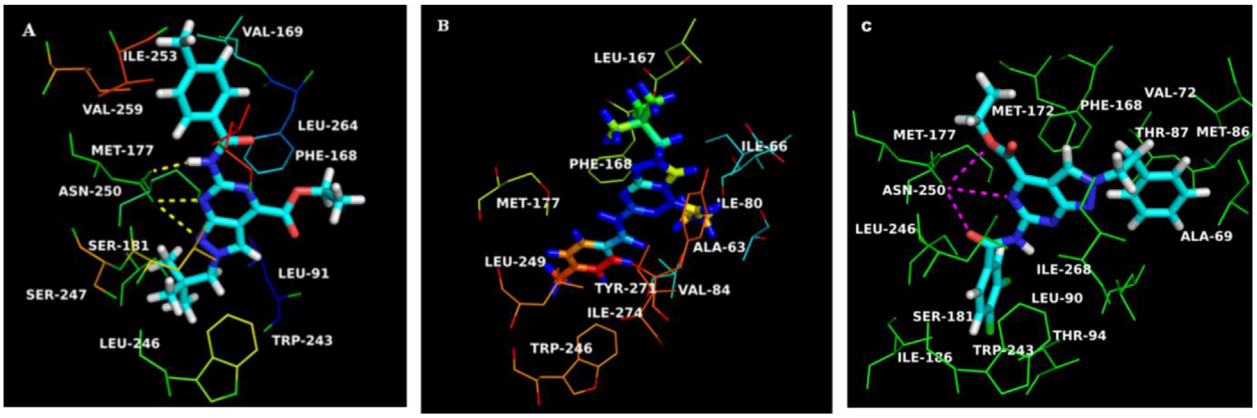

Fig. 4. A. Hypothetical binding mode of compound **5** obtained after docking simulations inside the hA_3AR binding site. **B**. Compound **5** inside the $hA_{2A}AR$ binding site. **C**. Hypothetical binding mode of compound **60** obtained after docking simulations inside the hA_3AR binding site. Poses are viewed from the membrane side facing TM6, TM7, and TM1.

(**55**–**60**) oriented in the same fashion as N^2 isopropyl derivatives and were involved in common hydrophobic interactions and lone hydrogen bonding interactions with Asn250. However, compound **60** of this series made 3 additional stabilizing hydrogen bonding interactions with Asn250 (Fig. 4-C). Similarly, compound **60** mimics the binding pose of compound **5** of previous work and was also involved in similar binding interactions such as hydrophobic interactions (Val169, Ile253, Val259 and Leu264), hydrogen bonding interaction (Asn250) and π-π stacking interaction (Phe168). In addition, the phenylethyl chain enabled the essential hydrophobic interactions with Trp243, Leu90, and Ser181. In fact, compound **60** displayed an affinity value of 2.2 μM at the hA_3AR.

Generally, dibenzamide substituted compounds (**61**, **63** & **65**) moved away from the binding site, and oriented deeply into the intracellular loop while the ligands were flipped to opposite direction as of ligand **60**, i.e. the pyrazole towards the TM6 (instead of TM3) and the pyrimidine towards the TM3 (instead of TM6).

We also docked the newly synthesized compounds inside the hA_{2A} binding pocket. We noticed that most of the compounds shared similar binding pose inside the binding pocket. In addition, the most potent and selective compound of the series, compound **5**, showed quite a opposite binding orientation inside the hA_{2A} binding pocket (Fig. 4-B) as compared to hA_3AR and failed to make hydrophobic interaction with essential residues such as Glu169 and barely made contact with Asn253, which is essential for the hA_{2A} antagonist activity. Some of the common hydrophobic residues observed around the ligands are Ala63, Ile80, Val84, Leu85, Trp246 and Tyr271.

The docking pose of the compound **5** was also compared with the most potent PTP compound (Figure S-1). The binding orientations of both the ligands are slightly different. However, compound **5** is oriented in the same plane as PTP. Interestingly, there is a trend observed between the binding pose of the PTP and compound **5**. The phenyl ring of the benzamide linkage in the PP is aligned over the phenyl ring of the PTP, thereby the PP has retained the essential hydrophobic interactions with residues such as Met177, Leu246 and Leu264 and Trp243, which are observed at the phenyl ring of PTP. Moreover, the ester chain of **5** was aligned over N^8 methyl group of the PTP counterpart, thus retaining the interaction with residues associated with N^8 methyl of PTPs. Finally, the N^2-neopentyl group in PP was aligned over the phenylacetamide chain of the PTP and involved in the hydrophobic interactions common to the phenylacetamide chain of PTP. These findings signify that most of the hydrophobic interactions associated with PTP are retained in the PP ligands as well.

In summary, docking evaluations were carried out on both homology-based hA_3AR and crystallographic $hA_{2A}AR$. Different binding orientation was observed for the ligands in the both binding pockets, which differ based on the substituents at C^6 and N^2 positions. As mentioned earlier, the binding pattern of compounds bearing N^2-neopentyl derivatives are slightly different from the other N^2substituted analogues because of the steric hindrance produced by the neopentyl groups inside the hA_3AR model and $hA_{2A}AR$.

Generally, docking studies confirmed that the most potent compounds of the PP-4-carboxylate series possessed better hA_3AR affinity due to stabilizing hydrogen bonding interactions with the Asn250, and displayed some specific hydrophobic interactions with Val169, Val259 and Ile253. These hydrogen bonding and hydrophobic interactions have contributed to the hA_3AR affinity and selectivity to a considerable extent. In addition, most of the newly synthesized derivatives showed a common binding orientation pattern throughout the series inside the $hA_{2A}AR$, with the exception of some compounds, which were bound in a slightly different fashion due to the substituents effects such as electronic properties, positional effects and rotatable nature. This resulted in compounds showing common interactions (which include the hydrogen bonding interactions with Asn253) and other hydrophobic interactions essential for $hA_{2A}AR$ activation. Thus, some compounds showed good affinity towards the $hA_{2A}AR$ as well and subsequent poor selectivity.

3. Conclusions

In summary, we have synthesized and characterized a new series of simplified pyrazolo[3,4-*d*]pyrimidine-4-carboxylate derivatives using an efficient synthetic procedure. The previously reported compounds **4** and **5**, bearing the N^2-neopentyl moiety and a *para*-CF_3 and *para*-CH_3 benzamido groups at the C^6 position, remained the most potent and selective hA_3AR antagonists of the PP series. In addition, the exploration of new substituents at the N^2 and C^6 position of the nucleus led to the discovery of new derivatives, such as compounds **60** and **62**, which displayed good affinity at the hA_3AR (**60**, K_i $hA_3AR = 2.2$ μM; **62**, K_i $hA_3AR = 2.9$ μM) and a significant selectivity towards the other AR subtypes (**60**, >46; **62**, >34). Even if the binding data make it difficult to elaborate a clear SAR profile, we can conclude that the presence of an ethyl ester and of a substituted benzamido group at the C^4 and C^6 positions, respectively, in combination with a bulky group at the N^2 position (such as neopentyl (**4**, **5**, **54**) or phenylethyl (**57**–**60**)), led to good affinity towards hA_3AR. In some cases (e.g. **4**, **5** & **60**) the compounds showed good selectivity towards the hA_3AR. A little alkyl group at the N^2 position, such as methyl, was tolerated only when a sterically hindered moiety was concurrently present at the C^6 position (**62**). Docking studies confirmed the pharmacological data: compounds **4**, **5**, **60** and **62** inside the binding pocket of the hA_3AR displayed interactions with key residues, such as Asn250 (**4**, **5**, **60**, **62**), Phe168 (**4**, **5**, **62**), Val169 (**4**, **5**) and Leu264 (**4**, **5**, **62**). Moreover, these simplified analogues were able to overcome the limitations typically associated with the tricyclic PTP structures, such as high molecular weight and lipophilicity.

4. Experimental

4.1. Chemistry

Reactions were routinely monitored by thin-layer chromatography (TLC) on silica gel plate (precoated 60 F_{254} Merck plate). Column chromatographies were performed using silica gel 60 (Merck, 70-230 mesh). Melting points were determined on a Gallenkamp instrument and were uncorrected. Compounds were dissolved in HPLC (high performance liquid chromatography) grade methanol for determination of mass to charge *m*/*z* on a LCQ Finnigan MAT mass spectrometer (source of ionization: Electrospray ionization (ESI) probe). ^1H and ^{13}C NMR spectra were determined in the deuterated dimethylsulfoxide (DMSO-d_6) solutions on Bruker DPX ultrashield NMR (400 MHz) spectrometers, with chemical shifts given in parts per million (δ) downfield relative to tetramethylsilane (TMS) as internal standard, and *J* values (coupling constants) given in hertz. The following abbreviations were used: s, singlet; d, doublet; t, triplet; sep, septet; m, multiplet; br, broad.

HPLC Studies: The purity of the compounds was determined *via* analytical HPLC using HITACHI, *version* 3.1.8b on a Phenomenex Gemini 5U C18 column (5 μM, 110 Å, 150 mm × 4.60 mm i.d.) at room temperature at a flow rate of 1.0 mL/min with two different mobile phase eluent systems at 254 nm UV detection. The isocratic elution was followed and analysis was carried out using mobile phase eluent systems ACN (65%): H_2O.

*4.1.1. General procedure for the synthesis of 3-amino-1-alkyl or arylalkyl-1H-pyrazole-4-carbonitriles (**6**–**9**)*

To a solution of 3-amino-1*H*-pyrazole-4-carbonitrile (1.08 g, 0.01 mol) in anhydrous DMF (5 ml), anhydrous potassium carbonate (1.65 g, 0.012 mol, 1.2 equiv) was added at 0 °C and the resulting mixture was stirred at the same temperature for 45 min. Appropriate alkyl/aryl iodide or bromide (0.012 mol, 1.2 equiv) was added slowly over 15 min and the reaction mixture was heated at 90 °C for 10 h. Then the resulting reaction mixture was cooled, poured over ice cold water and the aqueous phase was extracted with EtOAc (3 × 10 ml), the combined organic layers were dried over Na_2SO_4, filtered, and the solvent was removed under reduced pressure to give an oily residue that was purified via column chromatography eluting with a mixture of hexane/ethylacetate (1:1) to obtain the desired products (**6**–**9**) as solids.

*4.1.1.1. 3-Amino-1-methyl-1H-pyrazole-4-carbonitrile (**6**).* Pale yellow solid, mp 125–127 °C (0.723 g, 67%). ^{1}H NMR (400 MHz, DMSO-d_6): δ 3.52 (s, 3H, N-CH_3), 6.53 (s, 2H, NH_2), 7.51 (s, 1H, pyrazole-*H*). ^{13}C NMR (400 MHz, DMSO-d_6): δ 35.0 (N–CH_3), 72.6 (C–CN), 115.7 (CN), 140.3 (CH), 151.9 (C–NH_2). LC–MS (ESI) analysis (*m*/*z*) calcd for $C_5H_6N_4$ (122.13): found 122.8 $[M+H]^+$.

*4.1.1.2. 3-Amino-1-isopropyl-1H-pyrazole-4-carbonitrile (**7**).* Pale yellow solid, mp 120–122 °C (0.745 g, 69%). ^{1}H NMR (400 MHz, DMSO-d_6): δ 1.33 (d, J = 6.64 Hz, 6H, $2CH_3$), 4.24 (sep, J = 6.64 Hz, 1H, CH), 5.52 (s, 2H, NH_2), 8.10 (s, 1H, pyrazole-*H*). LC–MS (ESI) analysis (*m*/*z*) calcd for $C_7H_{10}N_4$ (150.18): found 151.0 $[M+H]^+$.

*4.1.1.3. 3-Amino-1-neopentyl-1H-pyrazole-4-carbonitrile (**8**).* Pale yellow solid, mp 123–125 °C (0.766 g, 71%). ^{1}H NMR (400 MHz, DMSO-d_6): δ 0.89 (s, 9H, $3CH_3$), 3.67 (s, 2H, CH_2), 5.50 (s, 2H, NH_2), 8.04 (s, 1H, pyrazole-*H*). LC–MS (ESI) analysis (*m*/*z*) calcd for $C_9H_{14}N_4$ (178.23): found 179.2 $[M+H]^+$.

*4.1.1.4. 3-Amino-1-phenethyl-1H-pyrazole-4-carbonitrile (**9**).* Pale yellow solid, mp 132–134 °C (0.820 g, 76%). ^{1}H NMR (400 MHz, DMSO-d_6): δ 3.03 (t, J = 7.16 Hz, 2H, CH_2), 4.11 (t, J = 7.16 Hz, 2H, CH_2), 5.57 (s, 2H, NH_2), 7.13–7.29 (m, 5H, Ar–H), 7.92 (s, 1H, pyrazole-*H*). LC–MS (ESI) analysis (*m*/*z*) calcd for $C_{12}H_{12}N_4$ (212.25): found 213.0 $[M+H]^+$, 235.0 $[M+Na]^+$.

*4.1.2. General procedure for synthesis of 3-amino-1-(alkyl or aryl alkyl)-1H-pyrazole-4-carboxamide (**10**–**13**)*

Carbonitriles **6**–**9** (0.03 mol) were dissolved in 7 ml conc. H_2SO_4 at 0 °C and stirred at room temperature for 5 h. Then the reaction mixtures were poured into ice cold water and neutralized to pH 7 with 28% NH_3 solution. The white precipitates were formed which were further washed with cold water and dried under vacuum.

*4.1.2.1. 3-Amino-1-methyl-1H-pyrazole-4-carboxamide (**10**).* White solid, mp 155–157 °C (3.0 g, 83%). ^{1}H NMR (400 MHz, DMSO-d_6): δ = 3.50 (s, 3H, N–CH_3), 6.12 (s, 2H, NH_2), 6.64 (br s, 1H, NH), 7.16 (br s, 1H, NH), 7.59 (s, 1H, pyrazole-*H*). LC–MS (ESI) analysis (*m*/*z*) calcd for $C_5H_8N_4O$ (140.14): found 140.9 $[M+H]^+$.

*4.1.2.2. 3-Amino-1-isopropyl-1H-pyrazole-4-carboxamide (**11**).* White solid, mp 159–161 °C (3.82 g, 85%). ^{1}H NMR (400 MHz, DMSO-d_6): δ = 1.34 (d, J = 6.52 Hz, 6H, $2CH_3$), 4.18 (sep, J = 6.64 Hz, 1H, CH), 5.34 (s, 2H, NH_2), 6.69 (br s, 1H, NH), 7.16 (br s, 1H, NH), 7.94 (s, 1H, pyrazole-*H*). LC–MS (ESI) analysis (*m*/*z*) calcd for $C_7H_{12}N_4O$ (168.20): found 169.0 $[M+H]^+$.

*4.1.2.3. 3-Amino-1-neopentyl-1H-pyrazole-4-carboxamide (**12**).* White solid, mp 161–163 °C (4.17 g, 78%). ^{1}H NMR (400 MHz, DMSO-d_6): δ = 0.90 (s, 9H, $3CH_3$), 3.64 (s, 2H, CH_2), 5.32 (s, 2H, NH_2), 6.72 (br s, 1H, NH), 7.21 (br, 1H, NH), 7.85 (s, 1H, pyrazole-H). LC–MS (ESI) analysis (*m*/*z*) calcd for $C_9H_{16}N_4O$ (196.25): found 197.1 $[M+H]^+$.

*4.1.2.4. 3-Amino-1-phenethyl-1H-pyrazole-4-carboxamide (**13**).* White solid, mp 166–168 °C (5.73 g, 90%). ^{1}H NMR (400 MHz, DMSO-d_6): δ = 3.08 (t, J = 7.16 Hz, 2H, CH_2), 4.12 (t, J = 7.16 Hz, 2H, CH_2), 5.44 (s, 2H, NH_2), 6.24 (br s, 1H, NH), 6.74 (br s, 1H, NH), 7.19–7.35 (m, 5H, Ar–H), 7.80 (s, 1H, pyrazole-*H*). LC–MS (ESI) analysis (*m*/*z*) calcd for $C_{12}H_{14}N_4O$ (230.27): found 231.0 $[M+H]^+$, 254.2 $[M+Na]^+$.

*4.1.3. General procedure for synthesis of 3-(3-benzoylthioureido)-1-(alkyl or aryl alkyl)-1H-pyrazole-4-carboxamide (**14**–**17**)*

To a solution of carboxamides **10**–**13** (0.015 mol) in dry acetone (10 ml), benzoyl isothiocyanate (0.0165 mol, 1.1 equiv) was added and refluxed at 60 °C for 12 h. The reaction mixture was cooled. The resulting yellow solid was filtered, washed with acetone and dried under vacuum. The crude product was further recrystallized from methanol to obtain a pure solids.

*4.1.3.1. 3-(3-Benzoylthioureido)-1-methyl-1H-pyrazole-4-carboxamide (**14**).* Yellow solid, mp 218–220 °C (1.28 g, 61%). ^{1}H NMR (400 MHz, DMSO-d_6): δ = 3.61 (s, 3H, N–CH_3), 7.17 (br s, 1H, NH), 7.46–7.60 (m, 5H, Ar–H), 7.73 (d, 2H, $CONH_2$), 7.78 (s, 1H, pyrazole-*H*), 11.47 (br s, 1H, NH). LC–MS (ESI) analysis (*m*/*z*) calcd for $C_{13}H_{13}N_5O_2S$ (303.34): found 304.0 $[M+H]^+$.

*4.1.3.2. 3-(3-Benzoylthioureido)-1-isopropyl-1H-pyrazole-4-carboxamide (**15**).* Yellow solid, mp 212–214 °C (1.58 g, 63%). ^{1}H NMR (400 MHz, DMSO-d_6): δ = 1.42 (d, J = 5.76 Hz, 6H, $2CH_3$), 4.44–4.50 (m, 1H, CH), 7.07 (br, 1H, NH), 7.57–7.68 (m, 5H, Ar–H), 8.00 (d, 2H, $CONH_2$), 8.31 (s, 1H, pyrazole-*H*), 11.06 (br s, 1H, NH). LC–MS (ESI) analysis (*m*/*z*) calcd for $C_{15}H_{17}N_5O_2S$ (331.39): found 332.0 $[M+H]^+$.

*4.1.3.3. 3-(3-Benzoylthioureido)-1-neopentyl-1H-pyrazole-4-carboxamide (**16**).* Yellow solid, mp 215–217 °C (1.76 g, 60%). ^{1}H NMR (400 MHz, DMSO-d_6): δ = 0.91 (s, 9H, $3CH_3$), 3.91 (s, 2H, CH_2), 7.09 (brs, 1H, NHCO), 7.57–7.70 (m, 5H, Ar–H), 8.00 (d, 2H, $CONH_2$), 8.18 (brs, 1H, pyrazole-*H*). LC–MS (ESI) analysis (*m*/*z*) calcd for $C_{17}H_{21}N_5O_2S$ (359.45): found 360.2 $[M+H]^+$.

*4.1.3.4. 3-(3-Benzoylthioureido)-1-phenethyl-1H-pyrazole-4-carboxamide (**17**).* Yellow solid, mp 208–210 °C (2.44 g, 71%). ^{1}H NMR (400 MHz, DMSO-d_6): δ = 3.07 (br d, 2H, CH_2), 4.34 (br s, 2H, CH_2), 7.21–7.27 (m, 5H, Ar–H), 7.49–7.69 (m, 5H, Ar–H), 7.99 (s, 2H, $CONH_2$), 8.01 (s, 1H, pyrazole-*H*), 11.51 (br s, 1H, NHCO), 12.7 (br s, 1H, NH). LC–MS (ESI) analysis (*m*/*z*) calcd for $C_{20}H_{19}N_5O_2S$ (393.46): found 393.9 $[M+H]^+$.

*4.1.4. General procedure for synthesis of (E)-methyl N'-benzoyl-N-(4-carbamoyl-1-(alkyl or aryl alkyl)-1H-pyrazol-3-yl) carbamimidothioate (**18**–**21**)*

To a solution of benzoylthioureidos **13**–**17** (0.003 mol) in 10 ml of 0.1 N NaOH, methyl iodide (0.0036 mol, 1.2 equiv) was added at room temperature and the resulting mixture was stirred for 3 h. The white suspension was observed and it was adjusted to pH 6 with glacial acetic acid. The white precipitate was obtained, which was filtered and washed with cold water and finally dried under vacuum.

*4.1.4.1. (E)-Methyl-N'-benzoyl-N-(4-carbamoyl-1-methyl-1H-pyrazol-3-yl) carbamimidothioate (**18**).* White solid, mp 196–198 °C

(0.682 g, 75%). ^{1}H NMR (400 MHz, DMSO-d_6): δ = 2.44 (s, 3H, SCH_3), 3.57 (s, 3H, NCH_3), 7.42–7.52 (m, 5H, Ar–H), 7.70 (br s, 1H, pyrazole-*H*), 7.78 (d, 2H, $CONH_2$), 11.52 (br s, 1H, NH). LC–MS (ESI) analysis (*m*/*z*) calcd for $C_{14}H_{15}N_5O_2S$ (317.37): found 318.1 $[M+H]^+$.

*4.1.4.2. (E)-Methyl-N'-benzoyl-N-(4-carbamoyl-1-isopropyl-1H-pyrazol-3-yl)carbamimidothioate (**19**).* White solid, mp 223–225 °C (0.665 g, 67%). ^{1}H NMR (400 MHz, DMSO-d_6): δ = 1.45 (d, *J* = 6.52 Hz, 6H, $2CH_3$), 2.41 (s, 3H, SCH_3), 4.59 (br s, 1H, CH), 7.39–7.91 (m, 5H, Ar–H), 8.02 (d, 2H, $CONH_2$), 8.24 (s, 1H, pyrazole-*H*), 13.09 (br s, 1H, NH). LC–MS (ESI) analysis (*m*/*z*) calcd for $C_{16}H_{19}N_5O_2S$ (345.42): found 346.0$[M+H]^+$.

*4.1.4.3. (E)-Methyl-N'-benzoyl-N-(4-carbamoyl-1-neopentyl-1H-pyrazol-3-yl)carbamimidothioate (**20**).* White solid, mp 219–221 °C (0.600 g, 56%). ^{1}H NMR (400 MHz, DMSO-d_6): δ = 0.90 (s, 9H, $3CH_3$), 2.42 (s, 3H, SCH_3), 4.02 (s, 2H, CH_2), 7.40–7.95 (m, 5H, Ar–H), 8.02 (d, 2H, $CONH_2$), 8.17 (s, 1H, pyrazole-*H*). LC–MS (ESI) analysis (*m*/*z*) calcd for $C_{18}H_{23}N_5O_2S$ (373.47): found 374.1$[M+H]^+$, 396.2 $[M+Na]^+$.

*4.1.4.4. (E)-Methyl-N'-benzoyl-N-(4-carbamoyl-1-phenethyl-1H-pyrazol-3-yl)carbamimidothioate (**21**).* White solid, mp 235–237 °C (0.743 g, 63%). ^{1}H NMR (400 MHz, DMSO-d_6): δ = 2.41 (s, 3H, SCH_3), 3.13 (t, *J* = 7.04 Hz, 2H, CH_2), 4.45 (t, *J* = 7.04, Hz, 2H, CH_2), 7.11–7.23 (m, 5H, Ar–H), 7.39–7.87 (m, 5H, Ar–H), 8.00 (d, 2H, $CONH_2$), 8.12 (s, 1H, pyrazole-*H*), 13.10 (br s, 1H, NH). LC–MS (ESI) analysis (*m*/*z*) calcd for $C_{21}H_{21}N_5O_2S$ (407.49): found 408.2 $[M+H]^+$, 430.2 $[M+Na]^+$.

*4.1.5. General procedure for synthesis of (Z)-3-(2-benzoylguanidino)-1-(alkyl or aryl alkyl)-1H-pyrazole-4-carboxamide (**22**–**25**)*

Carbamimidothioate derivatives **18**–**21** (0.003 mol) were dissolved in dry DMF (5 ml) containing 2% ammonia (5 ml) and heated to 120 °C for 3 h in a sealed tube. At the end of the reaction the odour of methyl mercaptan was recognized, cooled and poured over ice water mixture. The resulting white precipitate was washed with water and dried under vacuum.

*4.1.5.1. (Z)-3-(2-Benzoylguanidino)-1-methyl-1H-pyrazole-4-carboxamide (**22**).* White solid, mp > 300 °C (0.504 g, 53%). Insoluble.

*4.1.5.2. (Z)-3-(2-Benzoylguanidino)-1-isopropyl-1H-pyrazole-4-carboxamide (**23**).* White solid, mp > 300 °C (0.642 g, 62%). Insoluble.

*4.1.5.3. (Z)-3-(2-Benzoylguanidino)-1-neopentyl-1H-pyrazole-4-carboxamide (**24**).* White solid, mp > 300 °C (0.627 g, 56%). Insoluble.

*4.1.5.4. (Z)-3-(2-Benzoylguanidino)-1-phenethyl-1H-pyrazole-4-carboxamide (**25**).* White solid, mp > 300 °C (0.646 g, 53%). Insoluble.

*4.1.6. General procedure for synthesis of 6-amino-2-(alkyl or aryl alkyl)-2H-pyrazolo[3,4-d]pyrimidin-4(5H)-one (**26**–**29**)*

A suspension of benzoylguanidino derivatives **22**–**25** (3.5 mmol) in 1 N NaOH (10 ml) was refluxed at 110 °C for 12 h. The resulting milky white mixture was adjusted to pH 6 with acetic acid. A mixture of benzoic acid and free amine derivatives were obtained which was washed with water and dried. Finely divided powder was suspended in hot ethanol with stirring to remove benzoic acid and filtered hot. The resulting ethanolic portion was evaporated to dryness to obtain a pure desired product as white solid.

*4.1.6.1. 6-Amino-2-methyl-2H-pyrazolo[3,4-d]pyrimidin-4(5H)-one (**26**).* White solid, mp > 300 °C (0.721 g, 72%). ^{1}H NMR (400 MHz, DMSO- d_6): δ = 3.69 (s, 3H, NCH_3), 6.69 (s, 2H, NH_2), 7.73 (s, 1H, pyrazole-*H*), 10.58 (s, 1H, NHCO). LC–MS (ESI) analysis (*m*/*z*) calcd for $C_6H_7N_5O$ (165.16): found 166.1 $[M+H]^+$.

*4.1.6.2. 6-Amino-2-isopropyl-2H-pyrazolo[3,4-d]pyrimidin-4(5H)-one (**27**).* White solid mp > 300 °C (0.825 g, 75%). ^{1}H NMR (400 MHz, DMSO- d_6): δ = 1.42 (d, *J* = 6.52 Hz, 6H, $2CH_3$), 4.50 (sep, *J* = 6.52 Hz, 1H, CH), 6.90 (s, 2H, NH_2), 8.11 (s, 1H, pyrazole-*H*), 10.61 (s, 1H, NHCO). LC–MS (ESI) analysis (*m*/*z*) calcd for $C_8H_{11}N_5O$ (193.21): found 194.2 $[M+H]^+$, 216.0 $[M+Na]^+$.

*4.1.6.3. 6-Amino-2-neopentyl-2H-pyrazolo[3,4-d]pyrimidin-4(5H)-one (**28**).* White solid, mp > 300 °C (0.815 g, 68%). ^{1}H NMR (400 MHz, DMSO-d_6): δ = 0.96 (s, 9H, $3CH_3$), 3.70 (s, 2H, CH_2), 6.24 (s, 2H, NH_2), 7.67 (s, 1H, pyrazole-*H*). LC–MS (ESI) analysis (*m*/*z*) calcd for $C_{10}H_{15}N_5O$ (221.26): found 222.0 $[M+H]^+$, 244.0 $[M+Na]^+$.

*4.1.6.4. 6-Amino-2-phenethyl-2H-pyrazolo[3,4-d]pyrimidin-4(5H)-one (**29**).* White solid, mp > 300 °C (1.067 g, 81%). ^{1}H NMR (400 MHz, DMSO-d_6): δ = 3.10 (t, *J* = 6.64 Hz, 2H, CH_2), 4.36 (t, *J* = 6.64 Hz, 2H, CH_2), 7.34 (s, 2H, NH_2), 7.14–7.30 (m, 5H, CH), 7.89 (s, 1H, pyrazole-*H*), 10.62 (s, 1H, NHCO). LC–MS (ESI) analysis (*m*/*z*) calcd for $C_{13}H_{13}N_5O$ (255.28): found 256.0 $[M+H]^+$, 278.0 $[M+Na]^+$.

*4.1.7. General procedure for synthesis of 4-chloro-2-(alkyl or arylalkyl)-2H-pyrazolo[3,4-d]pyrimidin-6-amine (**30**–**33**)*

A mixture of 6-amino-2-(alkyl or arylalkyl)-2*H*-pyrazolo[3,4-*d*]pyrimidin-4(5*H*)-ones (**26**–**29**) (0.005 mol), phosphoryl trichloride (0.1 mol, 20 equiv) and N,N-dimethylamine (0.005 mol, 1 equiv) was refluxed at 110 °C for 24 h. Then the reaction mixture was cooled and the excess phosphoryl trichloride was removed under reduced pressure. The resulting red oil was poured onto ice mixture slowly, stirred for 10 min and the aqueous part was extracted with EtOAc (3 × 10 ml). The combined organic layers were dried over Na_2SO_4, filtered, and the solvent was removed under reduced pressure to give an oily residue that was purified via column chromatography eluting with a mixture of hexane/ethylacetate (1:1) to obtain pale yellow solids as desired products (**30**–**33**).

*4.1.7.1. 4-Chloro-2-methyl-2H-pyrazolo[3,4-d]pyrimidin-6-amine (**30**).* Pale yellow solid, mp 247–249 °C (0.536 g, 65%). ^{1}H NMR (400 MHz, DMSO-d_6): = 4.00 (s, 3H, N–CH_3), 6.90 (s, 2H, NH_2), 8.43 (s, 1H, pyrazole-*H*). ^{13}C NMR (400 MHz, DMSO-d_6): δ = 33.9, 106.5, 132.2, 153.8, 156.1, 161.8. LC–MS (ESI) analysis (*m*/*z*) calcd for $C_6H_6ClN_5$ (183.60): found 184.3 $[M+H]^+$, 206.1 $[M+Na]^+$. HPLC purity (254 nm); 98.2%; eluent: 60% ACN:H_2O, t_R = 2.2 min.

*4.1.7.2. 4-Chloro-2-isopropyl-2H-pyrazolo[3,4-d]pyrimidin-6-amine (**31**).* Pale yellow solid, mp 151–153 °C (0.647 g, 67%). ^{1}H NMR (400 MHz, DMSO-d_6): δ = 1.48 (d, *J* = 6.64 Hz, 6H, $2CH_3$), 4.53 (sep, *J* = 6.64 Hz, 1H, CH), 6.18 (s, 2H, NH_2), 8.30 (s,1H, pyrazole-H). ^{13}C NMR (400 MHz, DMSO-d_6): δ = 22.0, 48.4, 106.7, 132.1, 153.7, 155.1, 166.6. LC–MS (ESI) analysis (*m*/*z*) calcd for $C_8H_{10}ClN_5$ (211.65): found 212.1 $[M+H]^+$. HPLC purity (254 nm); 96.8%; eluent: 60% ACN:H_2O, t_R = 3.3 min.

*4.1.7.3. 4-Chloro-2-neopentyl-2H-pyrazolo[3,4-d]pyrimidin-6-amine (**32**).* Pale yellow solid, mp 154–156 °C (0.815 g, 77%). ^{1}H NMR (400 MHz, DMSO-d_6): δ = 0.96 (s, 9H, $3CH_3$), 4.01 (s, 2H, CH_2), 7.29 (s, 2H, NH_2), 8.02 (s, 1H, pyrazole-*H*).^{13}C NMR (400 MHz, DMSO-d_6):

δ = 28.1, 33.7, 57.3, 106.2, 132.2, 153.9, 156.9, 161.8. LC–MS (ESI) analysis (*m*/*z*) calcd for $C_{10}H_{14}ClN_5$ (239.70): found 240.0$[M+H]^+$. HPLC purity (254 nm); 100%; eluent: 60% ACN:H_2O, t_R = 6.0 min.

*4.1.7.4. 4-Chloro-2-phenethyl-2H-pyrazolo[3,4-d]pyrimidin-6-amine (**33**).* Pale yellow solid, mp 146–148 °C (0.918 g, 72%). ^{1}H NMR (400 MHz, DMSO-d_6): δ = 3.10 (t, *J* = 6.95 Hz, 2H, CH_2), 4.38 (t, *J* = 6.95 Hz, 2H, CH_2), 7.10–7.22 (m, 5H, Ar–H), 7.26 (s, 2H, NH_2), 7.97 (s,1H, pyrazole-*H*). ^{13}C NMR (400 MHz, DMSO-d_6): δ = 35.0, 47.8, 106.5, 126.8, 128.8, 129.0, 132.4, 138.6, 153.8, 156.1, 161.7. LC–MS (ESI) analysis (*m*/*z*) calcd for $C_{13}H_{12}ClN_5$ (273.72): found 272.0 $[M-H]^-$. HPLC purity (254 nm); 99.3%; eluent: 60% ACN:H_2O, t_R = 5.5 min.

*4.1.8. General procedure for synthesis of 6-amino-2-(alkyl or aralkyl)-2H-pyrazolo[3,4-d]pyrimidine-4-carbonitrile (**34**–**37**)*

A mixture of 4-chloro-2-(alkyl or aralkyl)-2*H*-pyrazolo[3,4-*d*] pyrimidin-6-amines (**30**–**34**) (0.00054 mol), sodium cyanide (0.0011 mol, 2 equiv), sodium *p*-toluene sulfinate (0.00016 mol, 0.3 equiv) in 5 mL of anhydrous DMF was heated on an oil bath at 80 °C for 2 h. The resultant mixture was cooled, poured into ice water mixture and stirred for 10 min. The solid was collected by filtration, washed with water and recrystallized from dimethylformamide and methanol mixture to obtain the desired products (**34**–**37**) as solids.

*4.1.8.1. 6-Amino-2-methyl-2H-pyrazolo[3,4-d]pyrimidine-4-carbonitrile (**34**).* Pale yellow solid, mp 131–133 °C (65%). ^{1}H NMR (400 MHz, DMSO-d_6): δ = 3.88 (s, 3H, N–CH_3), 7.51 (s, 2H, NH_2), 8.24 (s, 1H, pyrazole-*H*). ^{13}C NMR (400 MHz, DMSO-d_6): δ = 33.7, 108.7, 115.1, 131.9, 135.3, 155.7, 162.2. LC–MS (ESI) analysis (*m*/*z*) calcd for $C_7H_6N_6$ (174.16): found 173.1 $[M-H]^-$.

*4.1.8.2. 6-Amino-2-isopropyl-2H-pyrazolo[3,4-d]pyrimidine-4-carbonitrile (**35**).* Pale yellow solid, mp 125–127 °C (77%). ^{1}H NMR (400 MHz, DMSO-d_6): δ = 1.47 (d, *J* = 6.64 Hz, 6H, $2CH_3$), 4.91 (sep, *J* = 6.64 Hz, 1H, CH), 7.46 (s, 2H, NH_2), 8.23 (s,1H, pyrazole-*H*). ^{13}C NMR (400 MHz, DMSO): δ = 21.9, 48.3, 109.1, 115.1, 131.8, 135.3, 154.8, 162.0. LC–MS (ESI) analysis (*m*/*z*) calcd for $C_9H_{10}N_6$ (202.22):found 201.1 $[M-H]^-$.

*4.1.8.3. 6-Amino-2-neopentyl-2H-pyrazolo[3,4-d]pyrimidine-4-carbonitrile (**36**).* Pale yellow solid, mp 148–150 °C (62%). ^{1}H NMR (400 MHz, DMSO-d_6): δ = 0.98 (s, 9H, $3CH_3$), 4.06 (s, 2H, CH_2), 7.48 (s, 2H, NH_2), 8.27 (s, 1H, pyrazole-*H*).^{13}C NMR (400 MHz, DMSO-d_6): δ = 28.1, 33.7, 57.2, 108.5, 115.1, 131.8, 135.4, 156.6, 162.3. LC–MS (ESI) analysis (*m*/*z*) calcd for $C_{11}H_{14}N_6$ (230.27): found 229.2 $[M-H]^-$.

*4.1.8.4. 6-Amino-2-phenethyl-2H-pyrazolo[3,4-d]pyrimidine-4-carbonitrile (**37**).* Pale yellow solid, mp 135–137 °C (81%). ^{1}H NMR (400 MHz, DMSO-d_6): δ = 3.14 (t, *J* = 7.16 Hz, 2H, CH_2), 4.44 (t, *J* = 7.16 Hz, 2H, CH_2), 7.12–7.26 (m, 5H, Ar–H), 7.43 (s, 2H, NH_2), 8.21 (s, 1H, pyrazole-*H*). ^{13}C NMR (400 MHz, DMSO-d_6): δ = 34.9, 47.6, 108.8, 115.0, 126.9, 128.8, 129.0, 132.1, 135.3, 138.5, 155.8, 162.2. LC–MS (ESI) analysis (*m*/*z*) calcd for $C_{14}H_{12}N_6$ (264.29): found 263.4 $[M-H]^-$.

*4.1.9. General procedure for synthesis of 6-amino-2-(alkyl or aralkyl)-2H-pyrazolo[3,4-d]pyrimidine-4-carboxamide (**38**–**41**)*

To a stirred solution of 6-amino-2-(alkyl or aralkyl)-2*H*-pyrazolo [3,4-*d*] pyrimidine-4-carbonitriles **34**–**37** (0.00057 mol) in DMSO (3 mL) at cold condition, 30% H_2O_2 (0.0023 mol, 4 equiv) and anhydrous K_2CO_3 (0.0011 mol, 2 equiv) were added. The mixture was stirred at room temperature for 1 h. Then the resultant mixture was poured into ice water mixture and stirred for 10 min. The solid was collected by filtration, washed with water and recrystallized from methanol to obtain the desired products (**38**–**41**) as solids.

*4.1.9.1. 6-Amino-2-methyl-2H-pyrazolo[3,4-d]pyrimidine-4-carboxamide (**38**).* White solid, mp > 300 °C (78%). ^{1}H NMR (400 MHz, DMSO-d_6): δ = 3.83 (s, 3H, N–CH_3), 7.03 (s, 2H, NH_2), 7.84 (br s, 1H, NH), 7.96 (br s, 1H, NH), 8.16 (s, 1H, pyrazole-*H*). LC–MS (ESI) analysis (*m*/*z*) calcd for $C_7H_8N_6O$ (192.18): found 191.4 $[M-H]^-$.

*4.1.9.2. 6-Amino-2-isopropyl-2H-pyrazolo[3,4-d]pyrimidine-4-carboxamide (**39**).* White solid, mp 177–179 °C (70%). ^{1}H NMR (400 MHz, DMSO-d_6): δ = 1.48 (d, *J* = 6.8 Hz, 6H, $2CH_3$), 4.93 (sep, *J* = 6.8 Hz, 1H, CH), 7.03 (s, 2H, NH_2), 7.90 (br s, 1H, NH), 7.98 (br s, 1H, NH), 8.23 (s, 1H, pyrazole-*H*). LC–MS (ESI) analysis (*m*/*z*) calcd for $C_9H_{12}N_6O$ (220.23): found 219.0 $[M-H]^+$.

*4.1.9.3. 6-Amino-2-neopentyl-2H-pyrazolo[3,4-d]pyrimidine-4-carboxamide (**40**).* White solid, mp 174–176 °C (79%). ^{1}H NMR (400 MHz, DMSO-d_6): δ = 0.99 (s, 9H, $3CH_3$), 4.07 (s, 2H, CH_2), 7.03 (s, 2H, NH_2), 7.89 (br s, 1H, NH), 8.00 (br s, 1H, NH), 8.24 (s, 1H, pyrazole-*H*). LC–MS (ESI) analysis (*m*/*z*) calcd for $C_{11}H_{16}N_6O$ (248.28): found 247.0 $[M-H]^-$.

*4.1.9.4. 6-Amino-2-phenethyl-2H-pyrazolo[3,4-d]pyrimidine-4-carboxamide (**41**).* Pale yellow solid, mp 182–184 °C (84%). ^{1}H NMR (400 MHz, DMSO-d_6): δ = 3.16 (br s, 2H, CH_2), 4.44 (br s, 2H, CH_2), 7.00 (s, 2H, NH_2), 7.16–7.25 (m, 5H, Ar–H), 7.85 (br s, 1H, NH), 7.96 (br s, 1H, NH), 8.19 (s, 1H, pyrazole-*H*). LC–MS (ESI) analysis (*m*/*z*) calcd for $C_{14}H_{14}N_6O$ (282.30): found 281.3 $[M-H]^+$.

*4.1.10. General procedure for synthesis of ethyl 6-amino-2-(alkyl or aralkyl)-2H-pyrazolo[3,4-d]pyrimidine-4-carboxylate (**42**–**45**)*

To a solution of 6-amino-2-(alkyl or aralkyl)-2*H*-pyrazolo[3,4-*d*] pyrimidine-4-carboxamides **38**–**41** (0.00052 mol) in absolute ethanol (30 mL), conc. H_2SO_4 (3 mL) was added slowly and the resulting mixture was refluxed at 80 °C for 12 h. The reaction mixture was cooled and excess ethanol was evaporated and the resulting oily residue was poured into ice water mixture, stirred for 10 min. The solid was collected by filtration, washed with water and recrystallized from methanol to obtain the desired products (**42**–**45**) as solids.

*4.1.10.1. Ethyl-6-amino-2-methyl-2H-pyrazolo[3,4-d]pyrimidine-4-carboxylate (**42**).* Pale brown solid, mp 155–156 °C (72%). ^{1}H NMR (400 MHz, DMSO-d_6): δ = 1.37 (t, *J* = 7.16 Hz, 3H, CH_3), 3.83 (s, 3H, N–CH_3), 4.42 (q, *J* = 7.10 Hz, 2H, CH_2), 7.26 (s, 2H, NH_2), 8.09 (s, 1H, pyrazole-*H*). ^{13}C NMR (400 MHz, DMSO-d_6): δ = 14.5, 33.6, 62.3, 106.4, 133.9, 150.8, 156.9, 162.4, 163.8. LC–MS (ESI) analysis (*m*/*z*) calcd for $C_9H_{11}N_5O_2$ (221.22): found 222.0 $[M+H]^+$. HPLC: purity (254 nm) 99.7%; t_R = 2.8 min.

*4.1.10.2. Ethyl-6-amino-2-isopropyl-2H-pyrazolo[3,4-d]pyrimidine-4-carboxylate (**43**).* Pale yellow solid, mp. 139–141 °C (75%). ^{1}H NMR (400 MHz, DMSO-d_6): δ = 1.37 (t, *J* = 7.16 Hz, 3H, CH_3), 1.43 (d, *J* = 6.76 Hz, 6H, $2CH_3$), 4.42 (q, *J* = 7.16 Hz, 2H, CH_2), 4.89 (sep, *J* = 6.76 Hz, CH), 7.22 (s, 2H, NH_2), 8.11 (s,1H, pyrazole-*H*). ^{13}C NMR (400 MHz, DMSO-d_6): δ = 14.5, 22.0, 47.9, 62.3, 106.6, 133.7, 151.0, 155.9, 162.4, 163.9. DEPT (400 MHz, DMSO-d_6): δ 14.5.

(CH_3), 22.0 (CH_3), 47.9 (CH-alkyl), 62.3 (CH_2), 133.7 (CH-pyrazole). LC–MS (ESI) analysis (*m*/*z*) calcd for $C_{11}H_{15}N_5O_2$ (249.27): found 250.1 $[M+H]^+$. HPLC: purity (254 nm) 100%; t_R = 2.7 min.

*4.1.10.3. Ethyl-6-amino-2-neopentyl-2H-pyrazolo[3,4-d]pyrimidine-4-carboxylate (**44**).* Pale yellow solid, mp. 120–122 °C (84%). ^{1}H NMR (400 MHz, DMSO-d_6): δ = 0.99 (s, 9H, 3CH$_3$), 1.43 (t, J = 7.0 Hz, 3H, CH$_3$), 4.07 (s, 2H, CH$_2$), 4.47 (q, J = 7.0 Hz, 2H, CH$_2$), 7.27 (s, 2H, NH$_2$), 8.18 (s, 1H, pyrazole-*H*).^{13}C NMR (400 MHz, DMSO-d_6): δ = 14.5, 28.2, 33.8, 57.0, 62.3, 106.0, 133.7, 151.0, 157.7, 162.7, 163.9. LC–MS (ESI) analysis (*m*/*z*) calcd for $C_{13}H_{19}N_5O_2$ (277.32): found 278.1 [M+H]$^+$. HPLC: purity (254 nm) 97.9%; t_R = 3.6 min.

*4.1.10.4. Ethyl-6-amino-2-phenethyl-2H-pyrazolo[3,4-d]pyrimidine-4-carboxylate (**45**).* Yellowish brown solid, mp 131–132 °C (88%). ^{1}H NMR (400 MHz, DMSO-d_6): δ = 1.37 (t, J = 6.96 Hz, 3H, CH$_3$), 3.15 (t, J = 6.84 Hz, 2H, CH$_2$), 4.39–4.46 (m, 4H, 2CH$_2$), 7.14–7.24 (m, 7H, Ar–H, NH$_2$), 8.11 (s, 1H, pyrazole-*H*). ^{13}C NMR (400 MHz, DMSO-d_6): δ = 14.5, 35.1, 47.5, 62.3, 106.4, 126.8, 128.8, 129.1, 133.9, 138.7, 151.0, 156.9, 162.6, 163.9. LC–MS (ESI) analysis (*m*/*z*) calcd for $C_{16}H_{17}N_5O_2$ (311.34): found 312.1 [M+H]$^+$. HPLC: purity (254 nm) 100%; t_R = 3.1 min.

*4.1.11. General procedure for synthesis of ethyl 6-benzamido-(alkyl or aralkyl)-2H-pyrazolo[3,4-d]pyrimidine-4-carboxylate (**46**–**60**)*

To a suspension of ethyl 6-amino-2-(alkyl or aralkyl)-2*H*-pyrazolo[3,4-*d*]pyrimidine-4-carboxylates **42**–**45** (0.00045 mol) in anhydrous toluene (5 mL), diisopropylethylamine (0.00135 mol, 3 equiv) and substituted benzoyl chlorides (0.00135 mol, 3 equiv) were added. The mixture was heated under reflux for 24 h. The solvent was removed under reduced pressure and the resulting residue was purified by column chromatography (hexane: EtOAc, 4:6) to obtain the desired products (**46**–**60**) as solids.

*4.1.11.1. Ethyl-6-benzamido-2-methyl-2H-pyrazolo[3,4-d]pyrimidine-4-carboxylate (**46**).* White solid, mp 107–109 °C (51%). ^{1}H NMR (400 MHz, DMSO-d_6): δ = 1.42 (t, J = 7.16 Hz, 3H, CH$_3$), 4.03 (s, 3H, N–CH$_3$), 4.50 (q, J = 7.16 Hz, 2H, CH$_2$), 7.51–8.03 (m, 5H, Ar–H), 8.45 (s, 1H, pyrazole-*H*), 11.47 (s, 1H, NH). ^{13}C NMR (400 MHz, DMSO-d_6): δ = 14.5, 34.2, 62.8, 109.9, 128.8, 128.9, 129.7, 132.7, 134.0, 150.8, 155.6, 156.2, 163.4, 166.3. LC–MS (ESI) analysis (*m*/*z*) calcd for $C_{16}H_{15}N_5O_3$ (325.32): found 326.1 [M+H]$^+$. HPLC: purity (254 nm) 100%; t_R = 3.0 min.

*4.1.11.2. Ethyl-6-(4-fluorobenzamido)-2-methyl-2H-pyrazolo[3,4-d]pyrimidine-4-carboxylate (**47**).* White solid, mp 103–105 °C (53%). ^{1}H NMR (400 MHz, DMSO-d_6): δ = 1.42 (t, J = 7.04 Hz, 3H, CH$_3$), 4.03 (s, 3H, N–CH$_3$), 4.50 (q, J = 7.04 Hz, 2H, CH$_2$), 7.34–8.11 (m, 4H, Ar–H), 8.45 (s, 1H, pyrazole-*H*), 11.52 (s, 1H, NH). LC–MS (ESI) analysis (*m*/*z*) calcd for $C_{16}H_{14}FN_5O_3$ (343.31): found 344.1 [M+H]$^+$. HPLC: purity (254 nm) 95.6%; t_R = 3.0 min.

*4.1.11.3. Ethyl-2-methyl-6-(4-(trifluoromethyl)benzamido)-2H-pyrazolo[3,4-d]pyrimidine-4-carboxylate (**48**).* White solid, mp 114–116 °C (55%). ^{1}H NMR (400 MHz, DMSO-d_6): δ = 1.42 (t, J = 7.16 Hz, 3H, CH$_3$), 4.02 (s, 3H, N–CH$_3$), 4.50 (q, J = 7.16 Hz, 2H, CH$_2$), 7.89–8.18 (m, 4H, Ar–H), 8.46 (s, 1H, pyrazole-*H*), 11.75 (s, 1H, NH). LC–MS (ESI) analysis (*m*/*z*) calcd for $C_{17}H_{14}F_3N_5O_3$ (393.35): found 394.1 [M+H]$^+$. HPLC: purity (254 nm) 98.4%; t_R = 5.9 min.

*4.1.11.4. Ethyl-2-methyl-6-(4-methylbenzamido)-2H-pyrazolo[3,4-d]pyrimidine-4-carboxylate (**49**).* White solid, mp 109–111 °C (58%). ^{1}H NMR (400 MHz, DMSO-d_6): δ = 1.42 (t, J = 7.16 Hz, 3H, CH$_3$), 2.40 (s, 3H, CH$_3$), 4.03 (s, 3H, N–CH$_3$), 4.50 (q, J = 7.16, 2H, CH$_2$), 7.33–7.95 (m, 4H, Ar–H), 8.44 (s, 1H, pyrazole-*H*), 11.38 (s, 1H, NH). LC–MS (ESI) analysis (*m*/*z*) calcd for $C_{17}H_{17}N_5O_3$ (339.35): found 340.1 [M+H]$^+$, 362.1 [M+Na]$^+$. HPLC: purity (254 nm) 100.0%; t_R = 3.7 min.

*4.1.11.5. Ethyl-6-benzamido-2-isopropyl-2H-pyrazolo[3,4-d]pyrimidine-4-carboxylate (**50**).* White solid, mp 115–117 °C (49%). ^{1}H NMR (400 MHz, DMSO-d_6): δ = 1.42 (t, J = 7.12 Hz, 3H, CH$_3$), 1.51 (d, J = 6.64 Hz, 6H, 2CH$_3$), 4.50 (q, J = 7.12 Hz, 2H, CH$_2$), 5.07 (sep, J = 6.64 Hz, 1H, CH), 7.51–8.02 (m, 5H, Ar–H), 8.45 (s, 1H, pyrazole-*H*), 11.44 (s, 1H, NH). LC–MS (ESI) analysis (*m*/*z*) calcd for $C_{18}H_{19}N_5O_3$ (353.38): found 354.1 [M+H]$^+$. HPLC: purity (254 nm) 100%; t_R = 4.0 min.

*4.1.11.6. Ethyl-6-(4-fluorobenzamido)-2-isopropyl-2H-pyrazolo[3,4-d]pyrimidine-4-carboxylate (**51**).* White solid, mp 107–109 °C (42%). ^{1}H NMR (400 MHz, DMSO-d_6): δ = 1.41 (t, J = 7.12 Hz, 3H, CH$_3$), 1.51 (d, J = 6.64 Hz, 6H, 2CH$_3$), 4.50 (q, J = 7.12 Hz, 2H, CH$_2$), 5.07 (sep, J = 6.64 Hz, 1H, CH), 7.33–8.10 (m, 4H, Ar–H), 8.45 (s, 1H, pyrazole-*H*), 11.49 (s, 1H, NH). ^{13}C NMR (400 MHz, DMSO-d_6): δ = 14.5, 22.1, 49.3, 62.7, 110.2, 115.6, 115.8, 131.6, 131.7, 133.9, 150.8, 154.5, 155.8, 163.4, 165.3. LC–MS (ESI) analysis (*m*/*z*) calcd for $C_{18}H_{18}FN_5O_3$ (371.37): found 372.1 [M+H]$^+$. HPLC: purity (254 nm) 97.7%; t_R = 4.3 min.

*4.1.11.7. Ethyl-2-isopropyl-6-(4-(trifluoromethyl)benzamido)-2H-pyrazolo[3,4-d]pyrimidine-4-carboxylate (**52**).* White solid, mp 128–130 °C (53%). ^{1}H NMR (400 MHz, DMSO-d_6): δ = 1.41 (t, J = 7.04 Hz, 3H, CH$_3$), 1.49 (d, J = 6.64 Hz, 6H, 2CH$_3$), 4.49 (q, J = 7.04 Hz, 2H, CH$_2$), 5.01 (sep, J = 6.64 Hz, 1H, CH), 7.88–8.15 (m, 4H, Ar–H), 8.46 (s, 1H, pyrazole-*H*), 11.72 (s, 1H, NH). LC–MS (ESI) analysis (*m*/*z*) calcd for $C_{19}H_{18}F_3N_5O_3$ (421.37): found 422.1 [M+H]$^+$. HPLC: purity (254 nm) 98.1%; t_R = 6.9 min.

*4.1.11.8. Ethyl-2-isopropyl-6-(4-methylbenzamido)-2H-pyrazolo[3,4-d]pyrimidine-4-carboxylate (**53**).* White solid, mp. 131–133 °C (51%). ^{1}H NMR (400 MHz, DMSO-d_6): δ = 1.42 (t, J = 7.16 Hz, 3H, CH$_3$), 1.51 (d, J = 6.76 Hz, 6H, 2CH$_3$), 2.40 (s, 3H, CH$_3$), 4.50 (q, J = 7.16 Hz, 2H, CH$_2$), 5.08 (sep, J = 6.76 Hz, 1H, CH), 7.32–7.94 (m, 4H, Ar–H), 8.45 (s, 1H, pyrazole-*H*), 11.36 (s, 1H, NH). LC–MS (ESI) analysis (*m*/*z*) calcd for $C_{19}H_{21}N_5O_3$ (367.40): found 368.1 [M+H]$^+$. HPLC: purity (254 nm) 98.1%; t_R = 5.0 min.

*4.1.11.9. Ethyl-6-(4-fluorobenzamido)-2-neopentyl-2H-pyrazolo[3,4-d]pyrimidine-4-carboxylate (**54**).* Pale yellow solid, mp 112–114 °C (57%). ^{1}H NMR (400 MHz, DMSO-d_6): δ = 0.96 (s, 9H, 3CH$_3$), 1.43 (t, J = 7.16 Hz, 3H, CH$_3$), 4.21 (s, 2H, CH$_2$), 4.49 (q, J = 7.16 Hz, 2H, CH$_2$), 7.33–8.09 (m, 4H, Ar–H), 8.48 (s, 1H, pyrazole-*H*), 11.49 (s, 1H, NH). LC–MS (ESI) analysis (*m*/*z*) calcd for $C_{20}H_{22}FN_5O_3$ (399.42): found 400.1[M+H]$^+$. HPLC: purity (254 nm) 98.9%; t_R = 6.6 min.

*4.1.11.10. Ethyl-2-neopentyl-6-(4-(trifluoromethyl)benzamido)-2H-pyrazolo[3,4-d]pyrimidine-4-carboxylate (**4**).* Pale yellow solid, mp 116–118 °C (61%). ^{1}H NMR (400 MHz, DMSO-d_6): δ = 0.99 (s, 9H, 3CH$_3$), 1.47 (t, J = 7.0 Hz, 3H, CH$_3$), 4.20 (s, 2H, CH$_2$), 4.55 (q, J = 7.02 Hz, 2H, CH$_2$), 7.93–8.20 (m, 4H, Ar–H), 8.53 (s, 1H, pyrazole-*H*), 11.76 (s, 1H, NH). LC–MS (ESI) analysis (*m*/*z*) calcd for $C_{21}H_{22}F_3N_5O_3$ (449.43): found 450.1[M+H]$^+$. HPLC: purity (254 nm) 100%; t_R = 8.0 min.

*4.1.11.11. Ethyl-6-(4-methylbenzamido)-2-neopentyl-2H-pyrazolo[3,4-d]pyrimidine-4-carboxylate (**5**).* Pale yellow solid, mp 97–99 °C (48%). ^{1}H NMR (400 MHz, DMSO-d_6): δ = 1.01 (s, 9H, 3CH$_3$), 1.48 (t, J = 7.16 Hz, 3H, CH$_3$), 2.45 (s, 3H, CH$_3$), 4.25 (s, 2H, CH$_2$), 4.55 (q, J = 7.16 Hz, 2H, CH$_2$), 7.36–7.98 (m, 4H, Ar–H), 8.51 (s,1H, pyrazole-*H*), 11.39 (s, 1H, NH). ^{13}C NMR (400 MHz, DMSO-d_6): δ = 14.5, 21.5, 28.1, 33.8, 57.8, 62.7, 109.4, 128.9, 129.3, 129.9, 131.7, 133.9, 142.8, 150.9, 156.3, 163.5, 166.3. LC–MS (ESI) analysis (*m*/*z*) calcd for $C_{21}H_{25}N_5O_3$ (395.45): found 396.2 [M+H]$^+$. HPLC: purity (254 nm) 100%; t_R = 7.1 min.

*4.1.11.12. Ethyl-6-benzamido-2-phenethyl-2H-pyrazolo[3,4-d]pyrimidine-4-carboxylate (**55**).* Pale yellow solid, mp 106–108 °C (57%). ^{1}H NMR (400 MHz, DMSO-d_6): δ = 1.48 (t, J = 7.16 Hz, 3H, CH_3), 3.34 (t, J = 7.28 Hz, 2H, CH_2), 4.56 (q, J = 7.16 Hz, 2H, CH_2), 4.72 (t, J = 7.28 Hz, 2H, CH_2), 7.22–7.32 (m, 5H, Ar–H), 7.57–8.08 (m, 5H, Ar–H), 8.49 (s, 1H, pyrazole-*H*), 11.51 (s, 1H, NH). LC–MS (ESI) analysis (*m*/*z*) calcd for $C_{23}H_{21}N_5O_3$ (415.44): found 416.1 $[M+H]^+$. HPLC: purity (254 nm) 99.7%; t_R = 3.3 min.

*4.1.11.13. Ethyl-6-(4-fluorobenzamido)-2-phenethyl-2H-pyrazolo[3,4-d]pyrimidine-4-carboxylate (**56**).* Pale yellow solid, mp 112–113 °C (56%). ^{1}H NMR (400 MHz, DMSO-d_6): δ = 1.42 (t, J = 7.12 Hz, 3H, CH_3), 3.25 (t, J = 7.20 Hz, 2H, CH_2), 4.49 (q, J = 7.12 Hz, 2H, CH_2), 4.65 (t, J = 7.20 Hz, 2H, CH_2), 7.16–7.25 (m, 5H, Ar–H), 7.33–8.10 (m, 4H, Ar–H), 8.42 (s, 1H, pyrazole-*H*), 11.49 (s, 1H, NH). LC–MS (ESI) analysis (*m*/*z*) calcd for $C_{23}H_{20}FN_5O_3$ (433.44): found 434.1 $[M+H]^+$. HPLC: purity (254 nm) 100%; t_R = 6.5 min.

*4.1.11.14. Ethyl-2-phenethyl-6-(4-(trifluoromethyl)benzamido)-2H-pyrazolo[3,4-d]pyrimidine-4-carboxylate (**57**).* Pale yellow solid, mp 105–107 °C (52%). ^{1}H NMR (400 MHz, DMSO-d_6): δ = 1.48 (t, J = 7.16 Hz, 3H, CH_3), 3.31 (t, J = 7.26 Hz, 2H, CH_2), 4.56 (q, J = 7.16 Hz, 2H, CH_2), 4.72 (t, J = 7.26 Hz, 2H, CH_2), 7.24–7.31 (m, 5H, Ar–H), 7.39–8.16 (m, 4H, Ar–H), 8.49 (s, 1H, pyrazole-*H*), 11.56 (s, 1H, NH). LC–MS (ESI) analysis (*m*/*z*) calcd for $C_{24}H_{20}F_3N_5O_3$ (483.44): found 483.1 $[M+]^+$. HPLC: purity (254 nm) 100%; t_R = 6.7 min.

*4.1.11.15. Ethyl-6-(4-methylbenzamido)-2-phenethyl-2H-pyrazolo[3,4-d]pyrimidine-4-carboxylate (**58**).* Pale yellow solid, mp 143–144 °C (50%). ^{1}H NMR (400 MHz, DMSO-d_6): δ = 1.47 (t, J = 7.16 Hz, 3H, CH_3), 2.45 (s, 3H, CH_3), 3.30 (t, J = 7.28 Hz, 2H, CH_2), 4.54 (q, J = 7.16 Hz, 2H, CH_2), 4.71 (t, J = 7.28 Hz, 2H, CH_2), 7.21–7.30 (m, 5H, Ar–H), 7.37–7.99 (m, 4H, Ar–H), 8.47 (s, 1H, pyrazole-*H*), 11.40 (s, 1H, NH). LC–MS (ESI) analysis (*m*/*z*) calcd for $C_{24}H_{23}N_5O_3$ (429.47): found 430.1 $[M+H]^+$. HPLC: purity (254 nm) 100%; t_R = 7.2 min.

*4.1.11.16. Ethyl-6-(4-bromobenzamido)-2-phenethyl-2H-pyrazolo[3,4-d]pyrimidine-4-carboxylate (**59**).* Pale yellow solid, mp 139–141 °C (67%). ^{1}H NMR (400 MHz, DMSO-d_6): δ = 1.42 (t, J = 7.04 Hz, 3H, CH_3), 3.25 (t, J = 7.16 Hz, 2H, CH_2), 4.49 (q, J = 7.04 Hz, 2H, CH_2), 4.65 (t, J = 7.16 Hz, 2H, CH_2), 7.16–7.52 (m, 5H, Ar–H), 7.81–8.19 (m, 4H, Ar–H), 8.43 (s, 1H, pyrazole-*H*), 11.59 (s, 1H, NH). LC–MS (ESI) analysis (*m*/*z*) calcd for $C_{23}H_{20}BrN_5O_3$ (493.07): found 494.0 $[M+H]^+$. HPLC: purity (254 nm) 97.9%; t_R = 10.3 min.

*4.1.11.17. Ethyl-6-(3,4-dichlorobenzamido)-2-phenethyl-2H-pyrazolo[3,4-d]pyrimidine-4-carboxylate (**60**).* Pale yellow solid, mp 147–149 °C (64%). ^{1}H NMR (400 MHz, DMSO-d_6): δ = 1.42 (t, J = 7.16 Hz, 3H, CH_3), 3.25 (t, J = 7.28 Hz, 2H, CH_2), 4.49 (q, J = 7.16 Hz, 2H, CH_2), 4.65 (t, J = 7.28 Hz, 2H, CH_2), 7.14–7.25 (m, 5H, Ar–H), 7.77–8.26 (m, 3H, Ar–H), 8.43 (s, 1H, pyrazole-*H*), 11.66 (s, 1H, NH). ^{13}C NMR (400 MHz, DMSO-d_6): δ = 14.5, 34.9, 48.3, 62.8, 110.0, 126.9, 128.8, 129.1, 130.9, 131.1, 131.4, 131.7, 134.2, 135.0, 138.4, 150.8, 155.4, 155.7, 163.3, 164.3. LC–MS (ESI) analysis (*m*/*z*) calcd for $C_{23}H_{19}Cl_2N_5O_3$ (483.09): found 484.1 $[M+]^+$. HPLC: purity (254 nm) 97.7%; t_R = 11.1 min.

*4.1.12. General procedure for synthesis of ethyl 6-(N-benzoylbenzamido)-2-methyl-2H-pyrazolo[3,4-d]pyrimidine-4-carboxylate (**61**–**65**)*

To a suspension of ethyl 6-amino-2-(alkyl or aralkyl)-2*H*-pyrazolo[3,4-*d*]pyrimidine-4-carboxylates **42**–**45** (0.00045 mol) in anhydrous toluene (5 mL), diisopropylethylamine (0.0027 mol, 6 equiv) and benzoyl chloride or substituted benzoyl chlorides (0.0027 mol, 6 equiv) were added. The mixture was heated under reflux for 24 h. The solvent was removed under reduced pressure and the resulting residue was purified by column chromatography (hexane: EtOAc, 4:6).

*4.1.12.1. Ethyl-6-(N-benzoylbenzamido)-2-methyl-2H-pyrazolo[3,4-d]pyrimidine-4-carboxylate (**61**).* White solid, mp. 105–107 °C (56%). ^{1}H NMR (400 MHz, DMSO-d_6): δ = 1.36 (t, J = 7.16 Hz, 3H, CH_3), 3.87 (s, 3H, N–CH_3), 4.43 (q, J = 7.16 Hz, 2H, CH_2), 7.47–7.83 (m, 10H, Ar–H), 8.53 (s, 1H, pyrazole-*H*). LC–MS (ESI) analysis (*m*/*z*) calcd for $C_{23}H_{19}N_5O_4$ (429.43): found 430.1 $[M+H]^+$. HPLC: purity (254 nm) 98.0%; t_R = 5.4 min.

*4.1.12.2. Ethyl-6-(4-bromo-N-(4-bromobenzoyl)benzamido)-2-methyl-2H-pyrazolo[3,4-d]pyrimidine-4-carboxylate (**62**).* White solid, mp. 128–130 °C (53%). ^{1}H NMR (400 MHz, DMSO-d_6): δ = 1.36 (t, J = 7.08 Hz, 3H, CH_3), 3.92 (s, 3H, N–CH_3), 4.43 (q, J = 7.08 Hz, 2H, CH_2), 7.40–8.05 (m, 8H, Ar–H), 8.56 (s, 1H, pyrazole-*H*). LC–MS (ESI) analysis (*m*/*z*) calcd for $C_{23}H_{17}Br_2N_5O_4$ (586.26): found 587.2 $[M+]^+$. HPLC: purity (254 nm) 95.5%; t_R = 13.0 min.

*4.1.12.3. Ethyl-6-(N-(3,4-difluorobenzoyl)-3,4-difluorobenzamido)-2-methyl-2H-pyrazolo[3,4-d]pyrimidine-4-carboxylate (**63**).* White solid, mp. 169–171 °C (59%). ^{1}H NMR (400 MHz, DMSO-d_6): δ = 1.36 (t, J = 7.16 Hz, 3H, CH_3), 3.92 (s, 3H, N–CH_3), 4.43 (q, J = 7.16 Hz, 2H, CH_2), 7.52–8.00 (m, 6H, Ar–H), 8.55 (s, 1H, pyrazole-*H*). LC–MS (ESI) analysis (*m*/*z*) calcd for $C_{23}H_{15}F_4N_5O_4$ (501.39): found 502.1 $[M+H]^+$. HPLC: purity (254 nm) 100.0%; t_R = 11.6 min.

*4.1.12.4. Ethyl-6-(N-benzoylbenzamido)-2-isopropyl-2H-pyrazolo[3,4-d]pyrimidine-4-carboxylate (**64**).* White solid, mp 140–142 °C (53%). ^{1}H NMR (400 MHz, DMSO-d_6): δ = 1.25 (d, J = 6.64 Hz, 6H, $2CH_3$), 1.37 (t, J = 7.04 Hz, 3H, CH_3), 4.45 (q, J = 7.04 Hz, 2H, CH_2), 4.79 (sep, J = 6.64 Hz, 1H, CH), 7.47–7.97 (m, 10H, Ar–H), 8.51 (s, 1H, pyrazole-*H*). LC–MS (ESI) analysis (*m*/*z*) calcd for $C_{25}H_{23}N_5O_4$ (457.48): found 458.1 $[M+H]^+$. HPLC: purity (254 nm) 99.7%; t_R = 8.0 min.

*4.1.12.5. Ethyl-6-(N-benzoylbenzamido)-2-phenethyl-2H-pyrazolo[3,4-d]pyrimidine-4-carboxylate (**65**).* Pale yellow solid, mp 157–159 °C (55%). ^{1}H NMR (400 MHz, DMSO-d_6): δ = 1.41 (t, J = 7.04 Hz, 3H, CH_3), 2.87 (t, J = 6.92 Hz, 2H, CH_2), 4.48 (q, J = 7.04 Hz, 2H, CH_2), 4.57 (t, J = 6.92 Hz, 2H, CH_2), 6.92–7.25 (m, 5H, Ar–H), 7.54–8.02 (m, 10H, Ar–H), 8.50 (s, 1H, pyrazole-*H*). LC–MS (ESI) analysis (*m*/*z*) calcd for $C_{30}H_{25}N_5O_4$ (519.55): found: 520.19 $[M+H]^+$. PLC purity (254 nm); eluent: 95.8%; t_R = 9.4 min.

*4.1.13. General procedure for synthesis of ethyl 2-(alkyl or aralkyl)-6-(2-phenylacetamido)-2H-pyrazolo[3,4-d]pyrimidine-4-carboxylate (**66**–**69**)*

To a suspension of ethyl-6-amino-2-(alkyl or aralkyl)-2*H*-pyrazolo[3,4-*d*]pyrimidine-4-carboxylates **42**–**45** (0.00045 mol) in anhydrous toluene (5 mL), diisopropylethylamine (0.00135 mol, 3 equiv) and phenylacetyl chloride (0.00135 mol, 3 equiv) were added. The mixture was heated under reflux for 24 h. The solvent was removed under reduced pressure and the resulting residue was purified by column chromatography (hexane: EtOAc, 4:6).

*4.1.13.1. Ethyl-2-methyl-6-(2-phenylacetamido)-2H-pyrazolo[3,4-d]pyrimidine-4-carboxylate (**66**).* White solid, mp 168–170 °C (49%). ^{1}H NMR (400 MHz, DMSO-d_6): δ = 1.42 (t, J = 7.16 Hz, 3H, CH_3), 3.87

(s, 2H, CH_2), 3.98 (s, 3H, N–CH_3), 4.49 (q, J = 7.16 Hz, 2H, CH_2), 7.24–7.38 (m, 5H, Ar–H), 8.39 (s,1H, pyrazole-*H*), 11.29 (s, 1H, NH). LC–MS (ESI) analysis (*m*/*z*) calcd for $C_{17}H_{17}N_5O_3$ (339.35): found: 340.1 $[M+H]^+$. HPLC: purity (254 nm) 100%; t_R = 3.8 min.

*4.1.13.2. Ethyl-2-isopropyl-6-(2-phenylacetamido)-2H-pyrazolo[3,4-d]pyrimidine-4-carboxylate (**67**).* White solid, mp 120–122 °C (45%). ^{1}H NMR (400 MHz, DMSO-d_6): δ = 1.41 (t, J = 7.16 Hz, 3H, CH_3), 1.49 (d, J = 6.64 Hz, 6H, $2CH_3$), 3.87 (s, 2H, CH_2), 4.49 (q, J = 7.16 Hz, 2H, CH_2), 5.04 (sep, J = 6.64 Hz, 1H, CH), 7.25–7.37 (m, 5H, Ar–H), 8.39 (s, 1H, pyrazole-*H*), 11.28 (s, 1H, NH). LC–MS (ESI) analysis (*m*/*z*) calcd for $C_{19}H_{21}N_5O_3$ (367.40): found 368.1 $[M+H]^+$. HPLC: purity (254 nm) 100%; t_R = 4.1 min.

*4.1.13.3. Ethyl-2-neopentyl-6-(2-phenylacetamido)-2H-pyrazolo[3,4-d]pyrimidine-4-carboxylate (**68**).* Pale yellow solid, mp 112–114 °C (47%). ^{1}H NMR (400 MHz, DMSO-d_6): δ = 0.97 (s, 9H, $3CH_3$), 1.46 (t, J = 7.16 Hz, 3H, CH_3), 3.92 (s, 2H, CH_2), 4.21 (s, 2H, CH_2), 4.53 (q, J = 7.16 Hz, 2H, CH_2), 7.28–7.41 (m, 5H, Ar–H), 8.45 (s, 1H, pyrazole-*H*), 11.30 (s, 1H; NH). LC–MS (ESI) analysis (*m*/*z*) calcd for $C_{21}H_{25}N_5O_3$ (395.45): found 396.2 $[M+H]^+$. HPLC: purity (254 nm) 99.9%; t_R = 5.7 min.

*4.1.13.4. Ethyl-2-phenethyl-6-(2-phenylacetamido)-2H-pyrazolo[3,4-d]pyrimidine-4-carboxylate (**69**).* Pale yellow solid, mp 141–143 °C (53%). ^{1}H NMR (400 MHz, DMSO-d_6): δ = 1.44 (t, J = 7.16 Hz, 3H, CH_3), 3.26 (t, J = 7.16 Hz, 2H, CH_2), 3.92 (s, 2H, CH_2), 4.51 (q, J = 7.16 Hz, 2H, CH_2), 4.65 (t, J = 7.16 Hz, 2H, CH_2), 7.16–7.31 (m, 5H, Ar–H), 7.35–7.41 (m, 5H, Ar–H), 8.41 (s, 1H, pyrazole-*H*), 11.28 (s, 1H; NH). LC–MS (ESI) analysis (*m*/*z*) calcd for $C_{24}H_{23}N_5O_3$ (429.47): found 430.1 $[M+H]^+$. HPLC: purity (254 nm) 100%; t_R = 7.7 min.

4.2. Binding assay and adenylyl cyclase activity assay

Binding experiments with respective tritiated radioligands at hA_1AR, $hA_{2A}AR$ and hA_3AR were carried out for 3 h at room temperature as described previously [33]. Nonspecific binding was determined in the presence of 1 mM theophylline for hA_1AR and 100 μM (R)-N^6-phenyliso-propyladenosine (R-PIA) for both $hA_{2A}AR$ and hA_3AR. Bound and free radioactivity was separated by filtering the assay mixture through Whatman GF/B glass-fibre filters using a Micro-Mate 196-cell harvester (Packard Instrument Company). The filter bound radioactivity was counted on Top Count (efficiency of 57%) with Micro-Scint 20. The K_i values were calculated from competition curves by nonlinear curve fitting with the program SCTFIT [34]. In the case of $hA_{2B}AR$, adenylyl cyclase experiments were carried out as described previously with minor modifications [33–35]. Membranes transfected with hA_{2B} receptor were incubated with 100 nM NECA, as well as 150,000 cpm of [α-^{32}P]ATP and tested compounds in different concentrations for 20 min in the incubation mixture without EGTA (ethylene glycoltetraacetic acid) and NaCl. The K_i values for concentration-dependent inhibition of NECA-mediated adenylyl cyclase activity caused by tested antagonists were calculated accordingly.

4.3. Computational methodologies

All modeling studies were carried out on a Intel(R) Core[TM] 2 Quad CPU Q9550, 2.83 GHz, 3.25 GB RAM, DELL system. Docking simulation, energy calculation and the analyses of docking poses were performed using the Molecular Operating Environment (MOE, version 2010.10) suite [36]. The software package MOPAC (version 7) [37] implemented in the MOE suite, was utilized for all quantum mechanical calculations. PyMOL molecular graphics system was used for graphical visualizations and manipulations [38].

4.4. Homology modeling

The crystallographic structure of human A_{2A} AR complexed with ZM-241385 as high affinity antagonist (PDB code: 3EML) [39] was employed to build up a homology model of the hA_3AR by using software Modeller version 9.11 [40–43]. The tip of the second extracellular loop (Gln148 to Ser156) is absent in the crystal structure of A_{2A} AR (PDB code: 3EML) and it was not modelled owing to weak experimental electron density. Such missing tip of the loop is spatially distinct from the ligand-binding site and most probably does not directly interact with the binding cavity, as reported in Jaakola et al. [39]. The refined model was validated using PROCHECK program in Protein Structure Validation Suite (PSVS) [44].

4.5. Molecular docking simulations

Ligand structures were built using MOE-builder tool [36] and were subjected to MMFF94x energy minimization until the rms of conjugate gradient was <0.05 kcal mol^{-1} Å^{-1}. Partial charges for the ligands were calculated using PM3/ESP methodology.

All ligands were docked into the hypothetical TM binding site of the hA_3AR model and that of the $hA_{2A}AR$ crystal structure by using the docking tool of the MOE suite [36]. In the MOE-Dock, the Alpha PMI placement method, followed by force field refinement and London dG scoring, were used for the docking runs. MOE-Dock performed 100 independent docking runs (100 for our specific case) and wrote the resulting conformations and their energies in a molecular database file. The resulting docked complexes were subjected to MMFF94x energy minimization until the rms of conjugate gradient was <0.1 kcal mol^{-1} Å^{-1}. Prediction of antagonist–receptor complex stability (in terms of corresponding pK_i value) and the quantitative analysis for non bonded intermolecular interactions (H-bonds, hydrophobic, electrostatic) were calculated and visualized using tools implemented in MOE suite [36].

Acknowledgements

This work was supported by the National University of Singapore, and Singapore Ministry of Education (MOE2009-T2-2-011 and R-398-000-068-112; NUS-FRC R-148-000-164-112 and NUS NUSAGE N-148-000-009-001). The authors would like to thank Sonja Kachler for her assistance and expertise in the pharmacological evaluation of the compounds.

Appendix A. Supplementary data

Supplementary data related to this article can be found at http://dx.doi.org/10.1016/j.ejmech.2015.01.046.

References

[1] K.A. Jacobson, P.J.M. Vangalen, M. Williams, Adenosine receptors – pharmacology, structure-activity-relationships, and therapeutic potential, J. Med. Chem. 35 (1992) 407–422.
[2] C.E. Muller, D. Shi, M. Manning, J.W. Daly, Synthesis of paraxanthine analogs (1,7-disubstituted xanthines) and other xanthines unsubstituted at the 3-position – structure-activity-relationships at adenosine receptors, J. Med. Chem. 36 (1993) 3341–3349.
[3] Q.Y. Zhou, C.Y. Li, M.E. Olah, R.A. Johnson, G.L. Stiles, O. Civelli, Molecular-cloning and characterization of an adenosine receptor – the A3 adenosine receptor, Proc. Natl. Acad. Sci. U. S. A. 89 (1992) 7432–7436.
[4] S.A. Poulsen, R.J. Quinn, Adenosine receptors: new opportunities for future drugs, Bioorg. Med. Chem. 6 (1998) 619–641.
[5] K.A. Jacobson, Z.G. Gao, Adenosine receptors as therapeutic targets, Nat. Rev. Drug Discov. 5 (2006) 247–264.
[6] B.B. Fredholm, A.P. Ijzerman, K.A. Jacobson, K.N. Klotz, J. Linden, International Union of Pharmacology. XXV. Nomenclature and classification of adenosine receptors, Pharmacol. Rev. 53 (2001) 527–552.

[7] B.B. Fredholm, A.P. IJzerman, K.A. Jacobson, J. Linden, C.E. Muller, International Union of Basic and Clinical Pharmacology. LXXXI. Nomenclature and classification of adenosine receptors-an update, Pharmacol. Rev. 63 (2011) 1–34.
[8] S.L. Cheong, S. Federico, G. Venkatesan, A.L. Mandel, Y.M. Shao, S. Moro, G. Spalluto, G. Pastorin, The A3 adenosine receptor as multifaceted therapeutic target: pharmacology, medicinal chemistry, and in silico approaches, Med. Res. Rev. 33 (2013) 235–335.
[9] C.E. Muller, K.A. Jacobson, Recent developments in adenosine receptor ligands and their potential as novel drugs, Bba-Biomembranes 1808 (2011) 1290–1308.
[10] S.L. Cheong, A. Dolzhenko, S. Katchler, S. Paoletta, S. Federico, B. Cacciari, A. Dolzhenko, K.N. Klotz, S. Moro, G. Spalluto, G. Pastorin, The significance of 2-furyl ring substitution with a 2-(para-substituted) aryl group in a new series of pyrazolo-triazolo-pyrimidines as potent and highly selective hA(3) adenosine receptors antagonists: new insights into structure-affinity relationship and receptor-antagonist recognition, J. Med. Chem. 53 (2010) 3361–3375.
[11] A. Maconi, G. Pastorin, T. Da Ros, G. Spalluto, Z.G. Gao, K.A. Jacobson, P.G. Baraldi, B. Cacciari, K. Varani, S. Moro, P.A. Borea, Synthesis, biological properties, and molecular modeling investigation of the first potent, selective, and water-soluble human A(3) adenosine receptor antagonist, J. Med. Chem. 45 (2002) 3579–3582.
[12] P.G. Baraldi, G. Saponaro, R. Romagnoli, M.A. Tabrizi, S. Baraldi, A.R. Moorman, S. Cosconati, S. Di Maro, L. Marinelli, S. Gessi, S. Merighi, K. Varani, P.A. Borea, D. Preti, Water-soluble pyrazolo[4,3-e][1,2,4]triazolo[1,5-c]pyrimidines as human A(3) adenosine receptor antagonists, J. Med. Chem. 55 (2012) 5380–5390.
[13] S.L. Cheong, S. Federico, G. Venkatesan, P. Paira, Y.M. Shao, G. Spalluto, C.W. Yap, G. Pastorin, Pharmacophore elucidation for a new series of 2-aryl-pyrazolo-triazolo-pyrimidines as potent human A(3) adenosine receptor antagonists, Bioorg. Med. Chem. Lett. 21 (2011) 2898–2905.
[14] R. Yadav, R. Bansal, S. Kachler, K.N. Klotz, Novel 8-(p-substituted-phenyl/benzyl)xanthines with selectivity for the A2A adenosine receptor possess bronchospasmolytic activity, Eur. J. Med. Chem. 75 (2014) 327–335.
[15] L. Zilbershtein-Shklanovsky, P. Kafri, Y. Shav-Tal, E. Yavin, B. Fischer, Development of fluorescent double-strand probes labeled with 8-(p-CF3-cinnamyl)-adenosine for the detection of cyclin D1 breast cancer marker, Eur. J. Med. Chem. 79 (2014) 77–88.
[16] L. Squarcialupi, V. Colotta, D. Catarzi, F. Varano, M. Betti, K. Varani, F. Vincenzi, P.A. Borea, N. Porta, A. Ciancetta, S. Moro, 7-Amino-2-phenylpyrazolo[4,3-d]pyrimidine derivatives: structural investigations at the 5-position to target human A(1) and A(2A) adenosine receptors. Molecular modeling and pharmacological studies, Eur. J. Med. Chem. 84 (2014) 614–627.
[17] S.L. Cheong, A.V. Dolzhenko, S. Paoletta, E.P. Lee, S. Kachler, S. Federico, K.N. Klotz, A.V. Dolzhenko, G. Spalluto, S. Moro, G. Pastorin, Does the combination of optimal substitutions at the C(2)-, N(5)- and N(8)-positions of the pyrazolo-triazolo-pyrimidine scaffold guarantee selective modulation of the human A(3) adenosine receptors? Bioorg. Med. Chem. 19 (2011) 6120–6134.
[18] K.A. Jacobson, A.M. Klutz, D.K. Tosh, A.A. Ivanov, D. Preti, P.G. Baraldi, Medicinal chemistry of the A_3 adenosine receptor: agonists, antagonists, and receptor engineering, Handb. Exp. Pharmacol. (2009) 123–159.
[19] P. Paira, M.J. Chow, G. Venkatesan, V.K. Kosaraju, S.L. Cheong, K.N. Klotz, W.H. Ang, G. Pastorin, Organoruthenium antagonists of human A3 adenosine receptors, Chem. Eur. J. 19 (2013) 8321–8330.
[20] G. Venkatesan, P. Paira, S.L. Cheong, K. Vamsikrishna, S. Federico, K.N. Klotz, G. Spalluto, G. Pastorin, Discovery of simplified N-2-substituted pyrazolo[3,4-d]pyrimidine derivatives as novel adenosine receptor antagonists: efficient synthetic approaches, biological evaluations and molecular docking studies, Bioorgan. Med. Chem. 22 (2014) 1751–1765.
[21] P.G. Baraldi, B. Cacciari, R. Romagnoli, G. Spalluto, S. Moro, K.N. Klotz, E. Leung, K. Varani, S. Gessi, S. Merighi, P.A. Borea, Pyrazolo[4,3-e]1,2,4-triazolo[1,5-c]pyrimidine derivatives as highly potent and selective human A(3) adenosine receptor antagonists: influence of the chain at the N-8 pyrazole nitrogen, J. Med. Chem. 43 (2000) 4768–4780.
[22] P.G. Baraldi, B. Cacciari, S. Moro, G. Spalluto, G. Pastorin, T. Da Ros, K.N. Klotz, K. Varani, S. Gessi, P.A. Borea, Synthesis, biological activity, and molecular modeling investigation of new pyrazolo[4,3-e]-1,2,4-triazolo[1,5-c]pyrimidine derivatives as human A(3) adenosine receptor antagonists, J. Med. Chem. 45 (2002) 770–780.
[23] H. Shenlin, PCT Int. Appl., WO 2011025927, (2011).
[24] M.P. Groziak, J.W. Chern, L.B. Townsend, Heterocyclic synthesis via a 1,3-dicyclohexylcarbodiimide-mediated cyclodesulfurative annulation reaction – new methodology for the preparation of guanosine and guanosine-type nucleoside analogs, J. Org. Chem. 51 (1986) 1065–1069.
[25] K. Kazaoka, H. Sajiki, K. Hirota, Synthesis of 6-substituted 9-benzyl-8-hydroxypurines with potential interferon-inducing activity, Chem. Pharm. Bull. 51 (2003) 608–611.
[26] T. Higashino, S. Yoshida, E. Hayashi, Purines. 5. Reaction of 9-phenyl-9h-purine-6-carbonitrile with nucleophilic-reagents, Chem. Pharm. Bull. 30 (1982) 4521–4525.
[27] C. Qi, PCT Int. Appl., WO 2012030924, (2012).
[28] A. Yamazaki, I. Kumashir, T. Takenish, Synthesis of guanosine and its derivatives from 5-amino-1-beta-D-ribofuranosyl-4-imidazolecarboxamide. I. Ring closure with benzoyl isothiocyanate, J. Org. Chem. 32 (1967) 1825.
[29] A. Miyashita, S. Sato, N. Taido, K. Tanji, E. Oishi, T. Higashino, Studies on pyrazolo[3,4-D]pyrimidine derivatives. 17. Reactions of 5-benzoyl-4,5-dihydro-6-methyl-1-phenyl-1h-pyrazolo[3,4-D]pyrimidine-4-carbonitrile (the 6-methylpyrazolopyrimidine Reissert compound), Chem. Pharm. Bull. 38 (1990) 230–233.
[30] O. Lenzi, V. Colotta, D. Catarzi, F. Varano, D. Poli, G. Filacchioni, K. Varani, F. Vincenzi, P.A. Borea, S. Paoletta, E. Morizzo, S. Moro, 2-Phenylpyrazolo[4,3-d]pyrimidin-7-one as a new scaffold to obtain potent and selective human A(3) adenosine receptor antagonists: new insights into the receptor-antagonist recognition, J. Med. Chem. 52 (2009) 7640–7652.
[31] J.H. Kim, J. Wess, A.M. Vanrhee, T. Schoneberg, K.A. Jacobson, Site-directed mutagenesis identifies residues involved in ligand recognition in the human a(2a) adenosine receptor, J. Biol. Chem. 270 (1995) 13987–13997.
[32] Z.G. Gao, A. Chen, D. Barak, S.K. Kim, C.E. Muller, K.A. Jacobson, Identification by site-directed mutagenesis of residues involved in ligand recognition and activation of the human A(3) adenosine receptor, J. Biol. Chem. 277 (2002) 19056–19063.
[33] K.N. Klotz, J. Hessling, J. Hegler, C. Owman, B. Kull, B.B. Fredholm, M.J. Lohse, Comparative pharmacology of human adenosine receptor subtypes – characterization of stably transfected receptors in CHO cells, N. S. Arch. Pharmacol. 357 (1998) 1–9.
[34] A. Delean, A.A. Hancock, R.J. Lefkowitz, Validation and statistical-analysis of a computer modeling method for quantitative-analysis of radioligand binding data for mixtures of pharmacological receptor subtypes, Mol. Pharmacol. 21 (1982) 5–16.
[35] K.N. Klotz, G. Cristalli, M. Grifantini, S. Vittori, M.J. Lohse, Photoaffinity-labeling of A1-adenosine receptors, J. Biol. Chem. 260 (1985) 4659–4664.
[36] MOE (Molecular Operating Environment), Version 2010.10, Chemical Computing Group Inc. (1010 Sherbrooke Street West, Suite 910, Montreal, Quebec H3A 2R7, Canada), http://www.chemcomp.com.
[37] J.J.P. Stewart, MOPAC 7, Fujitsu Limited, Tokyo, 1993.
[38] W.L. De Lano, The PyMOL Molecular Graphics System, De Lano Scientific, San Carlos, CA, USA, 2002. http://www.pymol.org.
[39] V.P. Jaakola, M.T. Griffith, M.A. Hanson, V. Cherezov, E.Y.T. Chien, J.R. Lane, A.P. IJzerman, R.C. Stevens, The 2.6 Angstrom crystal structure of a human A(2A) adenosine receptor bound to an antagonist, Science 322 (2008) 1211–1217.
[40] N. Eswar, B. Webb, M.A. Marti-Renom, M.S. Madhusudhan, D. Eramian, M.Y. Shen, U. Pieper, A. Sali, Comparative Protein Structure Modeling Using MODELLER, 2007. Current Protocols in Protein Science/Editorial Board, John E. Coligan [et al.], Chapter 2 Unit 2 9.
[41] M.A. Marti-Renom, A.C. Stuart, A. Fiser, R. Sanchez, F. Melo, A. Sali, Comparative protein structure modeling of genes and genomes, Annu. Rev. Biophys. Biom. 29 (2000) 291–325.
[42] A. Sali, T.L. Blundell, Comparative protein modeling by satisfaction of spatial restraints, J. Mol. Biol. 234 (1993) 779–815.
[43] A. Fiser, R.K.G. Do, A. Sali, Modeling of loops in protein structures, Protein Sci. 9 (2000) 1753–1773.
[44] A. Bhattacharya, R. Tejero, G.T. Montelione, Evaluating protein structures determined by structural genomics consortia, Proteins 66 (2007) 778–795.